NACA RM E54L28a

NACA

# RESEARCH MEMORANDUM

## STATIC SEA-LEVEL PERFORMANCE OF AN AXIAL-FLOW-COMPRESSOR TURBOJET ENGINE WITH AN AIR-COOLED TURBINE

By Reeves P. Cochran and Robert P. Dengler

Lewis Flight Propulsion Laboratory
Cleveland, Ohio

NATIONAL ADVISORY COMMITTEE
FOR AERONAUTICS
WASHINGTON

March 15, 1955
Declassified February 10, 1959

NATIONAL ADVISORY COMMITTEE FOR AERONAUTICS

RESEARCH MEMORANDUM

# STATIC SEA-LEVEL PERFORMANCE OF AN AXIAL-FLOW-COMPRESSOR TURBOJET ENGINE WITH AN AIR-COOLED TURBINE

By Reeves P. Cochran and Robert P. Dengler

## SUMMARY

An experimental investigation was conducted to determine the effect on engine performance of bleeding air from the discharge of a 12-stage axial-flow compressor to cool the turbine rotor blades of a turbojet engine. A current production model of the engine was modified for this investigation by the substitution of a split-disk turbine rotor with air-cooled corrugated-insert rotor blades for the standard rotor and by the addition of a compressor-discharge-bleed cooling-air supply system. The rotor blades were untwisted with an essentially constant chord and were fabricated from noncritical metals; the shell was made of Timken 17-22A(S) alloy steel and the base of SAE 4130. Both materials are about 96-percent iron.

The engine was operated over a range of corrected engine speeds from 5000 to 7930 rpm and a range of coolant-flow ratios from zero to 0.05 with an open jet nozzle. At a constant engine speed of 7000 rpm (approximate cruising speed, 88 percent of rated), a range of jet nozzle areas was investigated. Each increase of 1 percent in the coolant-flow ratio at constant-speed, fixed-jet-nozzle operation caused increases of about 2 percent in turbine-inlet temperature ratio with accompanying increases in specific thrust and thrust specific fuel consumption of about 2 percent and 1 percent, respectively. Comparison of the experimental results of this investigation with analytical results of a previous matching study on a similar engine showed agreement in the trend of changes in the engine performance parameters with cooling.

Operation at a constant speed of 7000 rpm over a range of jet nozzle areas indicated that, at a given turbine-inlet temperature ratio, increasing the coolant-flow ratio would cause a decrease in specific thrust and an increase in thrust specific fuel consumption. Analytical calculations showed that these losses due to cooling would decrease as turbine-inlet temperature and turbine efficiency increased.

Low turbine efficiencies over the entire speed range resulted in high turbine-inlet temperatures, poor starting, and low-speed accelerating characteristics; however, response to the controls from about 4500 to rated rpm was fair. Average blade temperatures measured during the investigation indicated that the noncritical corrugated-insert blade could be operated at 7000 rpm with a coolant-flow ratio of 0.01 and turbine-inlet temperature of 1868° R and have a safety factor of 2.3.

## INTRODUCTION

One of the factors affecting the desirability of utilizing turbine cooling in turbojet engines to permit operation at higher turbine-inlet temperatures or to permit operation with noncritical turbine materials is the effect on the engine performance of bleeding cooling air from the compressor. Analytical studies concerning these effects have been conducted by other investigators (refs. 1 to 3). It was shown that very large gains in performance are obtainable by permitting operation at increased turbine-inlet temperatures and that the incremental change in performance due to cooling losses at these increased temperatures was generally of small magnitude. In reference 4 a matching study of two modified-production engines was made which indicated that, if cooling were added to existing engines at current temperature levels, the effects on engine performance resulting from air cooling can be somewhat larger than at higher operating temperatures. In order to provide an experimental verification for the analytical procedures and to gain further information on the effects of air cooling the turbine (by using compressor bleed) on turbojet-engine performance, experimental tests were conducted over a range of static sea-level engine conditions on a modified-production-model turbojet engine operating at current turbine-inlet temperature levels.

At the time that fabrication of parts for the test engine was begun, there was wide interest in the conservation of critical materials in the turbine; consequently, the emphasis in the engine modification was to eliminate critical materials and not necessarily to increase permissible turbine-inlet temperatures. For this reason the air-cooled turbine rotor blades were fabricated of noncritical materials (shell, Timken 17-22A(S); base and inserts, SAE 4130). The rotor blades were untwisted, had a constant chord, and had a coolant-passage configuration that utilized corrugated fins to augment the internal heat-transfer surface area. The air-cooled rotor was of the split-disk type.

With the engine modified by substituting the preceding mentioned parts for production parts, it was possible to obtain engine performance data at approximately current turbine-inlet temperature levels for a range of engine conditions with cooling air bled from the compressor

discharge and, in addition, to gain experience in the operation of an air-cooled turbine with noncritical rotor blades. Although these data are not directly applicable to air-cooled engines operating at high turbine-inlet temperatures, they do provide an approximate check on analytical procedures to determine if present calculation methods for predicting air-cooled engine performance are adequate.

This report is concerned with the following:

(1) The magnitude of the variation in engine performance parameters at sea-level static conditions as various amounts of air were bled from the compressor discharge for cooling purposes

(2) Comparison of analytically predicted performance changes with experimentally measured values

(3) Some operational aspects of an engine under conditions of compressor bleed for turbine cooling.

The engine was operated with a fixed jet nozzle area over a range of coolant-flow ratios at corrected speeds from 5000 to rated (7930) rpm. Engine performance at 7000 rpm with several exhaust-nozzle areas was investigated.

## APPARATUS

A modified 12-stage axial-flow compressor engine was used in this investigation for the determination of the performance characteristics of a turbojet engine with an air-cooled turbine. The original turbine rotor was replaced by a split-disk air-cooled turbine rotor with blades of noncritical material. The air for rotor-disk and -blade cooling was bled from the compressor discharge. A schematic diagram of the engine showing the cooling-air flow paths and the instrumentation stations is presented in figure 1.

### Engine Modifications

Turbine rotor. - A study of various air-cooled turbine disk configurations is made in reference 5. The type of disk that appeared to be most practical for use in an engine not previously designed for turbine cooling was a split-disk arrangement with a downstream cooling-air supply; consequently, this design was incorporated in this engine. Figure 2 shows external and internal views of the rotor. The details of the mechanical design of this air-cooled turbine rotor are presented in reference 5.

The disks were machined from standard-production turbine-rotor forgings for this engine with the upstream or forward disk being integral with the turbine shaft. Although this air-cooled rotor was originally designed on the basis of noncritical materials, the composite production forgings which consisted of SAE 4340 for the hub section and Timken 16-25-6 for the rim section were used because of availability. A 4.0-inch-diameter hole was provided in the center of the downstream or rear half of the rotor for introduction of the cooling air (see fig. 2). In an effort to keep the relative elongation of the two disks to a minimum, metal was removed from the center of the forward half (see fig. 3) to simulate the cooling-air supply hole in the rear disk, as is discussed in reference 6. An integral cooling-air impeller was formed between the two halves of the rotor by machining matching radial passages in both halves of the rotor from a radius of 5.75 inches out to the base of the blades with one passage for each of the 72 blades (see fig. 2). An inducer section with 36 curved vanes was provided near the cooling-air inlet at the hub to accelerate the cooling air to the wheel velocity. These curved vanes were machined from a radius of 3.00 inches to a radius of 5.25 inches on the downstream half of the rotor only. The vanes were of sufficient height to span the axial distance between the two halves of the rotor between these radii. The open radial space between the inducer section and the radial passages provided for some equalization of the flow distribution and simplified machining procedures. The two halves of the rotor were bolted together with twenty-four 7/16-inch body-fit bolts with sufficient tension to ensure against leakage of the cooling air between the two halves of the disk at the rim. The bolts were buried in the vanes of the cooling-air impeller and thus did not constrict the flow of cooling air. Metal-to-metal contact between the two disks was provided only along the outer 3 inches of the disk radius to minimize machining difficulties.

Turbine stator and rotor blades. - The original aerodynamic design of this air-cooled turbine was made for application to an earlier model of the same type of production turbojet engine that was used for this investigation. This original design and the performance results of a scale model operated in cold air are presented in reference 7. On the basis of an unpublished analysis, this turbine design was adapted to the present model of the production engine by the expedient of resetting the stator-blade angle to permit passage of the mass flow of the present engine, which was about 8 percent greater than that of the previous model. The aerodynamic profiles of the stator and rotor blades were maintained the same as those reported in reference 7. This method of adapting an existing turbine design for application in a similar engine was not very satisfactory as will be discussed in the section Comparison of Analytical and Experimental Results.

The stator blades for this design were more twisted than for conventional designs in order to match the nontwisted rotor blades which

are described subsequently. The stator blades were individually cast of a heat-resistant alloy, Haynes Stellite 21, by a lost-wax casting process and were assembled into production shroud bands to form a welded nozzle diaphragm. The same number of stator blades (64) were used in this nozzle diaphragm as were used in the standard engine nozzle diaphragm.

The turbine rotor (shown in fig. 2) had 72 nontwisted blades of uniform camber and was designed to replace the solid-blade production rotor which had 96 blades. The turbine solidity at the pitch diameter was maintained the same in the air-cooled turbine as in the production turbine. This resulted in a blade chord of 2.25 inches. The blade span was 3.75 inches, which is about the same as that of the production engine. The nontwisted rotor blade was chosen for this turbine because of the simplicity of providing coolant passages in such a configuration. The aerodynamic characteristics of nontwisted-rotor-blade turbines are evaluated analytically in reference 8 and were to be approximately the same as those of a free-vortex turbine designed for the same service.

The results of an experimental investigation into the use of corrugated fins to augment the heat-transfer surface area (ref. 9) showed that this was a promising internal configuration for an air-cooled blade. This type of configuration was adapted to the present turbine-rotor-blade profile (see fig. 4) and is analyzed for cooling effectiveness and pressure-loss characteristics in reference 10 with favorable results.

From the results of the preliminary investigations and analyses, the aerodynamic and mechanical designs of the turbine rotor blade were developed. The cooling-air-passage configuration consisted of corrugations 0.17 inch in pitch and 0.10 inch in amplitude (see fig. 4) placed around the inside perimeter of the blade shell. The inner portion of the blade was blocked-off by an insert capped at the blade root. The blade shell was formed from a tapered wall tube (0.020 in. at the tip and 0.040 in. at the root) of Timken alloy 17-22A(S). The insert and corrugations were fabricated from 0.010-inch SAE 4130 sheet stock and the insert cap of 0.030-inch SAE 4130 sheet stock. The blade base was a bulb-root type (see fig. 4) and was precision cast of SAE 4130 to the approximate contour by a frozen-mercury process. Timken 17-22A(S) and SAE 4130 are about 96- and 97-percent iron, respectively, and they represent a large savings of critical materials used in present-day uncooled turbine rotor blades.

The blade shell, corrugations, insert, and insert cap were assembled in the blade base and the entire assembly was simultaneously furnace-brazed in a dry-hydrogen atmosphere. Copper was utilized in brazing the insert cap, insert, corrugations, and shell together; and Nicrobraz was used to braze the shell to the base. A Nicrobraz coating was applied to

the leading and trailing edges of the outer surface of the blade shell and, subsequent to the brazing operation, a chemically deposited nickel coating was applied to the entire blade. This protective-coating method to reduce erosion and corrosion of the noncritical blade material is discussed in reference 11. After brazing, the bulb-root configuration of the blade base was ground to the final contour with a crush-type grinding wheel. This bulb-root configuration is discussed in detail in reference 5, where it is referred to as a "single-lug" base. It is pointed out in this reference that the machining expense and complexity of this base design were less, but that the stress levels were generally higher than in other base designs considered for cooled turbine blades. A bulb-root configuration was chosen for this application because of the relative simplicity of machining the mounting slots in the rim of the rotor. In order to alleviate the stress concentration at the junction between the blade base and the blade shell, a small fillet of Eutectic 16 was puddled around the ledge formed by the top of the integral fillet in a manner similar to that discussed in reference 12.

Excessive quantities of Nicrobraz present in the shell-to-base joint during the furnace-brazing operation caused clogging of a considerable number of coolant passages within the blade base with the result that the blades were not completely satisfactory for the pressure-loss and heat-transfer studies which had originally been formulated for this turbine.

Cooling-air system. - Provisions were made to supply cooling air to the turbine rotor from either a compressor-discharge bleed-off or from the laboratory high-pressure air system (see fig. 1). Air was bled from the compressor discharge by means of four existing $2\frac{1}{2}$-inch-diameter ports located in the compressor rear frame. The air was routed into a common line for the purposes of control and measurement and was then separated into two lines leading to opposite sides of the tail cone. The supply line for the laboratory air joined the common compressor bleed line downstream of the bleed-air control station. Control valves in the two supply lines permitted separate or combined operation of the two systems or operation with no cooling air. A standard engine tail cone was modified to provide for the introduction of the cooling air through tubes in the tail-cone struts into a supply tube along the centerline of the tail cone and thence into the 4-inch-diameter hole in the rear face of the turbine disk (see fig. 3). The cooling-air-flow path within the tail cone was essentially the same as that of model C of reference 13. This tail-cone configuration was shown to be the most effective of those tested from a pressure-loss standpoint. The tail-cone cooling-air tube is centered inside a labyrinth seal on the rear face of the turbine rotor by means of an integral 4-vane "spider" which is piloted through two sealed bearings mounted on a spindle shaft extending from the central portion of the forward turbine disk (see figs. 2 and 3).

Because the pilot bearings were surrounded by relatively high-temperature air from the compressor discharge, it was necessary to cool them by circulating water in an annular chamber around the outer race of the bearings. The basic principles of the mechanical design of this tail-cone cooling-air piping system were the same as those described in reference 6, except that the forward end of the cooling tube was attached to the tips of the spider vanes instead of free floating and a braided bellows, believed to be more flexible than the bellows shown in reference 6, was utilized.

As a precautionary measure, the mounting flange for the tail cone was modified to provide a blow-out or rupture section of thin sheet metal (about 0.040 in. thick) above the tip of the turbine rotor blades in place of the heavy turbine shroud on the standard engine (see fig. 3). The purpose of this blow-out section was to permit the immediate escape of any rotor blade that failed during operation, thus reducing the possibility of damage to the remaining blades in the rotor.

## Instrumentation

In addition to the basic instrumentation required for normal operation of an engine, special instrumentation was used to measure quantities of particular interest to this investigation. The engine speed was regulated with the aid of a stroboscopic tachometer, and a chronometric tachometer was used to accurately measure the engine speed. The fuel flow to the engine was measured by means of calibrated rotameters, and the engine thrust was measured by a calibrated strain-gage thrust meter.

Pressures and temperatures. - The locations of pressure and temperature measuring stations are given in figure 1, and the distribution of measurements at these stations is shown in figure 5. The thermocouples located at stations 3, 4, and 5 were chromel-alumel while all the other thermocouples were iron-constantan. Temperatures at stations 1, 2, 4, and 5 were determined from the arithmetical averages of the thermocouples distributed circumferentially and radially at these measuring stations. The thermocouples at the turbine inlet, station 3, were used only for engine operation as they were located in the burner core and indicated temperatures that were much higher than the average turbine-inlet temperature. Because the thermocouples at this station were inadequate to obtain a representative average measured temperature, the turbine-inlet temperature was calculated by the method described in appendix B.

Temperatures were also measured on the turbine rotor blades and the turbine disks and in the cooling-air passages at the base of the blades. The locations of the blade and cooling-air thermocouples are shown in figure 6. The disk thermocouples were located at 3.0-, 7.0-, 9.5-, 11.4-, and 13.0-inch radii on both the forward and rear halves of the rotor.

All thermocouples on the rotating parts were chromel-alumel. The thermocouple leads extended from the measuring points through a 3/8-inch-diameter hole along the centerline of the turbine and compressor shafts to a slip-ring thermocouple pickup on the front of the engine (see fig. 1).

Pressures were measured with manometers in which mercury, tetrabromoethane, alkazine, or water were used as reference fluid depending upon the magnitude of the pressure. Radial distributions of total pressure were measured at a number of circumferential locations at stations 1, 2, 4, and 5. In addition, the radial distribution of static pressure was measured at station 1.

Air flow. - In order to accurately determine the effect of varying amounts of compressor bleed-off on the performance of the engine, extensive measurements were made of the main engine air flow and the auxiliary air flows at various places on the engine setup. Venturi meters, sharp-edge orifices, and pitot-static tubes were used to obtain these air-flow measurements. (Locations of the measuring stations are given in fig. 1.) The symbols identifying each component of the air flow are given in appendix A, and the methods of measuring these components are shown in appendix B.

Accuracy. - The accuracy of the measurements reported herein is estimated to be within the following limits:

| | |
|---|---|
| Engine speed, percent | ±0.5 |
| Fuel flow, percent | ±1 |
| Thrust, percent | ±1 |
| Pressure, in. Hg | ±0.10 |
| Air weight flows, percent | ±1 |
| Air temperature, $^{\circ}R$ | ±2 |
| Gas temperatures, $^{\circ}R$ | ±10 |

## PROCEDURE

In this investigation, when the engine was started, cooling air for the turbine was supplied from the laboratory high-pressure air system. After the engine reached an idling speed of approximately 3000 rpm, the cooling-air supply was shifted from the laboratory system to compressor bleed. No attempt was made to start or to shut-down the engine on compressor bleed air in the present investigation. The engine was operated at corrected speeds of approximately 5000, 6000, 7000, and 7930 rpm with the adjustable exhaust nozzle in the fully open position (exhaust-nozzle area, 2.40 sq ft). At each speed, except 7930 rpm, the coolant-flow ratio was varied from approximately 0.05 to a minimum (zero at 6000 and 7000 rpm) that would still provide a safe short-time operating blade temperature (approx. 1100° F). At a corrected speed of 7930 rpm, only one point

was obtained (coolant-flow ratio of approximately 0.03) because of excessive turbine-inlet temperatures (well above the permissible limit of 2060° R) which threatened to damage the burner transition section and combustion chambers. At a corrected engine speed of approximately 7000 rpm, runs were made at two additional exhaust-nozzle settings, 2.32 and 2.26 square feet, over a range of coolant-flow ratios.

All symbols used in this report are presented in appendix A; and the methods for obtaining the various component weight flows, turbine-inlet temperature, specific thrust, and thrust specific fuel consumption are indicated in appendix B.

## RESULTS AND DISCUSSION

### Effect of Cooling-Air Bleed on Engine Performance over Range of Engine Speeds with Fixed Jet Nozzle Area

A summary of the engine operating conditions covered in this investigation is given in table I. The effects on turbine-inlet temperature ratio, specific thrust, and thrust specific fuel consumption of various amounts of cooling air bled from the compressor discharge over a range of engine speeds at a fixed jet nozzle area of 2.40 square feet are presented in figures 7 to 9.

As shown in table I, zero coolant-flow ratios were obtained only at engine speeds of about 6000 and 7000 rpm, and the maximum coolant-flow ratio at all speeds (except rated speed) was approximately 0.05. Low turbine efficiencies (on the order of 74 percent) resulted in excessive turbine-inlet temperatures which prevented operation over a range of coolant-flow ratios at rated speed. The curves presented in figure 7 were extrapolated to give a range of coolant-flow ratios from zero to 0.06 as shown by the dashed lines. Because only one coolant-flow ratio was run at rated speed (7930 rmp), the curves drawn through this point were based on the general slope of the curves at lower engine speeds.

In figure 7(a) is shown the variation of turbine-inlet temperature ratio with coolant-flow ratio under these engine operating conditions. At a constant coolant-flow ratio, the turbine-inlet temperature level rose with increase in engine speed for the range of speeds shown, but at speeds lower than about 5000 rpm, the temperature increased with decrease in engine speeds. Turbine-inlet temperature ratio increased linearly with increase in coolant-flow ratio at all engine speeds. This increase in temperature is required to maintain engine speed with a turbine weight flow reduced by the bleeding of cooling air from the compressor and to pump the additional amount of cooling air through the rotor blades. From figure 7(a) it can be seen that at a corrected engine speed of 6963 rpm, each increase of 0.01 in coolant-flow ratio resulted in approximately a

2.4-percent increase in the turbine-inlet temperature ratio. Increases in turbine-inlet temperature ratio with coolant-flow ratio of the same order of magnitude occurred at other constant engine speeds from 5000 to rated rpm.

Accompanying the increased turbine-inlet temperature ratio caused by bleeding cooling air from the compressor were changes in specific thrust and thrust specific fuel consumption (TSFC) as shown in figures 7(b) and (c), respectively, for the same engine operating conditions. The specific thrust plotted in figure 7(b) was determined by the method described in appendix B. As would be expected, the thrust level increased with engine speed. It can also be seen that, at a given constant speed with a fixed jet nozzle area, the specific thrust increased linearly with increase in coolant-flow ratio for the range of coolant flows covered. At a constant engine speed, there was a negligible variation of compressor-inlet weight flow and compressor pressure ratio with coolant-flow ratio; therefore, changes in measured specific thrust shown in this figure are essentially changes in thrust alone. This increase in thrust is the result of increased velocity of the gas at the jet nozzle caused by the higher jet nozzle temperature and pressure. The percentage increase in specific thrust with each increase of 0.01 in coolant-flow ratio varied from about 1.88 percent at 4877 rpm to about 2.44 percent at 6963 rpm. At constant turbine-inlet temperature and constant speed, specific thrust would decrease with increased coolant-flow ratio. This case will be discussed in more detail in the section Effects of Turbine Efficiency and Temperature on Performance.

The thrust specific fuel consumption plotted in figure 7(c) was determined by the method described in appendix B. At a constant corrected engine speed with fixed jet nozzle area, TSFC increased linearly with increase in coolant-flow ratio. The fuel consumption $w_f$ increased to give the increased turbine-inlet temperature previously discussed. Although the thrust also increased with the coolant-flow ratio, the fuel consumption increased at a more rapid rate and therefore the thrust specific fuel consumption increased. Increases in TSFC of about 1/2 to 1 percent occurred at speeds between 5000 and 7000 rpm for each increase of 0.01 in coolant-flow ratio.

## Effect of Cooling-Air Bleed on Engine Performance at 88 Percent Rated Speed and Various Jet Nozzle Areas

The performance results obtained when operating the engine at a constant corrected engine speed of 7000 rpm over a range of coolant-flow ratios and jet nozzle areas are presented in figure 8. This speed is 88 percent of rated speed and is approximately cruising speed for this engine. In this investigation, it was desired to know the effect on engine

performance of bleeding cooling air from the compressor discharge over a range of turbine-inlet temperatures. In order to cover such a range of engine operating conditions, the jet nozzle area was varied. A reduction in jet nozzle area resulted in higher pressure levels downstream of the turbine and, consequently, a smaller turbine pressure ratio. In order for the turbine power output to remain high enough to drive the compressor at the desired speed, an increase in turbine-inlet temperature was required. The lines of constant jet nozzle area $A_6$ shown on figure 8 are the areas set during the experimental operation. The absolute values of the jet nozzle area are of no real significance within themselves, but they do show the range of operation from the maximum, or open, jet nozzle area (2.40 sq ft) to the minimum area (2.26 sq ft) investigated. This latter area was the smallest area which would permit continuous operation at maximum coolant-flow ratio (about 0.05) without exceeding the permissible turbine-inlet temperature limit of about 2060° R (see table I). The range of coolant-flow ratios presented in table I for the engine operating conditions investigated was extrapolated to cover a range from zero to 0.06 by the same method used for figure 7. Fairing of curves of the performance parameters and cross-plotting of these faired curves have resulted in some final values in figure 8 that deviate slightly from the values listed in table I.

In figure 8(a) is shown the variation of specific thrust with turbine-inlet temperature ratio at various jet nozzle areas and coolant-flow ratios and a constant corrected engine speed of 7000 rpm. At a constant turbine-inlet temperature ratio, specific thrust increases as the jet nozzle area is reduced because of higher gas velocities at the jet nozzle. These higher gas velocities are the combined effect of reduced jet nozzle area and of reduced coolant flow, which results in a lower turbine pressure ratio and therefore a higher pressure at the jet nozzle. Along a line of constant coolant-flow ratio, it can be seen that the turbine-inlet temperature ratio increased to counteract the reduction in turbine pressure ratio after the jet nozzle area decreased sufficiently to take the turbine out of limiting loading. This increase in temperature due to reduced nozzle area caused the specific thrust to rise. At a constant jet nozzle area, the changes in specific thrust and turbine-inlet temperature ratio are similar to those discussed in connection with figures 7(a) and (b).

The changes in corrected thrust specific fuel consumption with turbine-inlet temperature ratio for the range of engine operation previously described are shown in figure 8(b). At a constant coolant-flow ratio, reduction of jet nozzle area from the open position (2.40 sq ft) resulted in an initial decrease in TSFC with very little change in turbine-inlet temperature ratio. These trends in temperature and fuel consumption indicate that the turbine was probably in a condition of limiting loading with the jet nozzle open. Further reduction in the jet nozzle area at constant coolant-flow ratio caused an increase in turbine-inlet temperature ratio with an accompanying increase in TSFC as would

normally be expected in this type of engine operation. At a constant turbine-inlet temperature ratio and decreasing jet nozzle area, the decrease in TSFC with decreasing coolant-flow ratio was due to the increase in thrust shown in figure 8(a) for the same conditions. The changes in TSFC with coolant-flow ratio at a constant jet nozzle area were similar to those discussed in connection with figure 7(c).

## Comparison of Analytical and Experimental Results

The results of an analytical matching study to determine the effect of a compressor-discharge bleed-off for turbine cooling on the performance of an engine similar to the present experimental engine are reported in reference 4. A comparison of these results with data from the present investigation was made over a range of coolant-flow ratios at an engine speed of 6963 rpm and a jet nozzle area of 2.40 square feet in an attempt to check analytical methods of predicting the performance of an engine under these operating conditions. The results of this comparison are shown in figure 9. The experimental curves for parts (a), (b), and (c) of figure 9 are taken from parts (a), (b), and (c) of figure 7, respectively, of this report.

Because of certain differences in the two engines, the main one being turbine efficiency, these comparisons can be treated only as indications of relative effects of cooling on engine performance. For the analytical calculations, the turbine efficiency was on the order of 79 percent (based on the cold-air results of ref. 7), whereas an efficiency of only 74 percent was determined in the present investigation. Changing the stator-blade setting to permit higher mass flow (as described previously) resulted in mismatching of the compressor and turbine and possibly moved the turbine operating point into a region of limiting loading with the resultant low efficiencies.

Another factor which possibly adversely affected the turbine efficiency of the experimental engine was the large clearance between the tip of the turbine rotor blades and the inner diameter of the blade blow-out section. This clearance was set proportionally higher on the experimental engine than on the cold-air scale model (ref. 7) for mechanical reasons because of the range of operating temperatures involved. In addition, the high operating temperature of the experimental engine caused differential expansions which further increased this clearance. The effect of this large clearance space, which permitted the combustion gases to leak past the turbine, was to reduce the effective turbine weight flow with a resultant increase in required turbine-inlet temperature and a decrease in turbine efficiency.

The effects of reduced turbine weight flow and low turbine efficiency can be seen from the equation for total turbine work:

$$\Delta H_t = w_3 \eta_t c_p T_3' \left[ 1 - (p_4'/p_3')^{\frac{\gamma-1}{\gamma}} \right] \quad (1)$$

Equation (1) shows that to maintain a given value of total turbine work $\Delta H_t$, when the turbine weight flow $w_3$ and turbine efficiency $\eta_t$ are reduced and the pressure ratio $p_4'/p_3'$ remains essentially constant, requires an increase in turbine-inlet temperature $T_3'$. The amount of this increase in temperature required to compensate for the low turbine efficiency and reduced turbine weight flow in the present engine is shown in the comparison of absolute values of the experimental and analytical turbine-inlet temperature ratios shown in figure 9(a). Although there is a difference in the level of the absolute values of the temperature ratios, it can be seen that the relative effect of cooling on the temperature ratio is practically the same for both cases.

As a result of the higher temperature level, the specific-thrust level for the experimental case was higher than that for the analytical case on the similar engine (see fig. 9(b)). However, the relative effect of cooling on specific thrust is very similar for the two cases.

A comparison between the experimental and analytical values of thrust specific fuel consumption on the two similar engines is shown in figure 9(c). The levels of the absolute values of TSFC are also different because of the difference in turbine-inlet temperature levels. Comparison of the relative effects of cooling on TSFC for the two cases shows that cooling caused a slightly greater increase in TSFC for the analytical case.

In general, all the comparisons in figure 9 show that the measured relative effects of cooling on engine performance agree in trend with those predicted analytically. The differences in the absolute values of the performance parameters shown in this figure are due to difference in matching characteristics of the two engines.

## Effects of Turbine Efficiency and Temperature on Performance

The experimental results presented herein have shown how variations in compressor-discharge bleed-off for turbine cooling affect the performance of one particular engine with the component efficiencies and turbine-inlet temperature range experienced during the experiment. Poor component matching and low turbine efficiency in the engine investigated resulted in relatively high thrust specific fuel consumption and high specific thrust

values for the range of engine speeds and turbine-inlet temperatures covered. Because the turbine efficiency and the turbine-inlet temperature level were much lower in the experimental engine than would probably be utilized in a future engine designed for air cooling, the performance variations experienced with this engine due to turbine cooling cannot be readily used in their present form to predict the operation that would be obtained with a high-temperature, high-performance engine. The performance variations presented herein are much inferior to what could be expected of this latter engine. In order to illustrate this, analytical comparisons are presented in figure 10 to show the separate effect of turbine-inlet temperature level and turbine efficiency level on the performance variations resulting from cooling of the turbine with compressor-discharge bleed-off. In this analytical comparison, the compressor operation is fixed at the point corresponding to zero coolant flow at 7000 rpm with the experimental engine.

From a designer's point of view, an engine will probably be designed for a specified turbine-inlet temperature, and the compressor and turbine will be matched for operation at this temperature for a given quantity of compressor bleed-off for turbine cooling. For this reason figure 10 is presented for the case where turbine-inlet temperature does not vary with coolant-flow ratio. The curves show the effect of design coolant-flow ratio on engine performance, relative to the case with no cooling air. The calculations for this analysis were made by the method detailed in reference 14. Two constant turbine-inlet temperatures were chosen for the comparison. The first was 1760° R, which is equal to the temperature encountered in the present engine with zero coolant-flow ratio at 7000 rpm, and the second was 2500° R, which is representative of the proposed temperature levels of future engines where turbine cooling will be a necessity. In combination with the specified temperatures, turbine efficiencies of 74 percent, the efficiency of the present turbine, and 85 percent, a value representative of good current and future engine design, were used.

It can be seen from the results of these calculations plotted in figure 10 that, with a constant turbine-inlet temperature of 1760° R, each percent of cooling caused a decrease of about 0.02 and 0.03 in specific-thrust ratio for turbine efficiencies of 85 and 74 percent, respectively, and increases of about 0.01 and 0.025 in thrust-specific-fuel-consumption ratio for the same two cases. The better performance of a high-efficiency turbine is obvious.

If the turbine-inlet temperature level were raised to 2500° R, it can be seen from figure 10 that for both efficiency cases each 1 percent of cooling air will cause only about 1-percent decrease in specific thrust while the thrust specific fuel consumption remains practically constant. The effect of turbine efficiency is much less pronounced at this temperature than at the low-temperature level. It is obvious from these comparisons that the engine performance of this investigation would be much

improved if mismatching of components had not caused such low turbine efficiencies. By referring to the trends in the values of relative performance parameters shown in figure 10, it can be seen that the low turbine efficiency and resulting high turbine-inlet temperature of the experimental engine caused two counteracting changes in performance. Low efficiency caused greater losses in specific thrust and higher TSFC, while higher temperatures resulted in lower specific-thrust losses and lower TSFC. From the comparison of the analytical and experimental data plotted in figure 9, it would appear that these counteracting effects very nearly compensate for each other, so that the engine performance with cooling relative to the case of no cooling is practically the same for the two cases.

## Some Operational Aspects of the Engine

As cooling of turbine rotor blades with air bled from the compressor is a relatively new field, some aspects of the operating characteristics of an engine under these conditions should be of interest. This air-cooled engine was a provisional modification of an existing production-model engine, and therefore its operating characteristics would not be necessarily representative of an engine which was initially designed to incorporate a compressor bleed system for air cooling of the turbine. However, such things as the levels of blade and disk temperatures, amounts of cooling air required, wearing qualities of the noncritical blades, and so forth, are of general interest as indications of the behavior of such components in any air-cooled engine.

The starting and low-speed acceleration characteristics of the engine were unsatisfactory due to the mismatching of the turbine with the compressor, which resulted in the poor aerodynamic efficiency of the turbine tested. Some changes in the standard controls system for the engine were found to be necessary for improving the low-speed operation. At speeds above 4500 rpm, the engine responded well to throttle advances and operated smoothly over the range of speeds from 5000 to about 7500 rpm, although the engine temperature levels were much higher than the design value due to low turbine efficiencies over the entire speed range.

The turbine rotor blades, which were fabricated of noncritical materials consisting of about 96-percent iron, were operated for a total of about 52 hours (of which the operations tabulated in table I are only a part) in this engine at speeds from idle to rated and coolant-flow ratios from zero to 0.05. During this range of operations, turbine-inlet temperatures from 1511° to 2314° R (1051° to 1854° F) were encountered. The maximum temperature of 2314° R at rated speed of 7930 rpm was held for only a 10- or 15-minute duration. Overheating of engine parts such as combustion chambers and associated sections prevented sustained operation at this temperature and speed. Reference 15 gives

an indication of the design provisions necessary for continuous operation of an engine at such elevated temperatures with sufficient cooling protection to all parts of the engine. The major portion of the experimental testing on this engine was done at 7000 rpm, where turbine-inlet temperatures from 1761° to 2039° R (1301° to 1579° F) were encountered. Visual inspection of the noncritical rotor blades at the completion of 52 hours of operation showed no evidence of elongation, distortion, surface erosion, cracking, or other physical failure. Some of the chemically deposited nickel coating and puddled-on fillets at the shell-to-base joint were lost during operation, but apparently with no adverse effect to the blades.

As has been mentioned in the APPARATUS section, errant braze material caused severe blockage of the cooling passages in these blades, and efforts to remove this material were only partially successful. As a result of this obstruction to the cooling-air flow in the blades, the cooling effectiveness was greatly impaired and the blade temperatures were higher than they would have been otherwise. Therefore, the temperatures measured on the rotor blades during this investigation do not reveal the true merits of the cooling characteristics of this type of blade configuration. These temperatures will be presented herein, however, to give the general range of blade temperatures obtained and to illustrate the effect of cooling on blade temperatures and the effect of blade temperatures of a noncritical blade material on the required coolant-flow ratio and therefore the operating point of the engine.

The variation of measured average turbine rotor-blade temperatures with turbine-inlet temperature over the range of coolant-flow ratios at 7000 rpm is presented in figure 11. The range of operation was extrapolated to the same extent and by the same method used for figure 8. Because of the possible variation of temperatures between blades due to the coolant-air passage blockage, only general bands of blade temperature at various coolant-flow ratios are indicated. The line of limiting permissible turbine-inlet temperature ratio (about 3.96) shown on the figure represents the turbine-inlet temperature of 2060° R previously described as the limit set for continuous engine operation. This limit was determined by parts of the engine other than the turbine rotor blades. The line labeled "stress ratio factor, 2.3" at a blade temperature level of 1120° F was the limiting operating temperature set for the air-cooled blades. In reference 12, a stress-ratio factor (ratio of the average allowable blade stress-rupture strength to blade average centrifugal stress) of 2.3 was recommended in the absence of more detailed design data as a tentative design criterion for air-cooled shell-supported blades made of Timken 17-22A(S). Other materials could conceivably permit much lower stress-ratio factors (higher stresses), but this value represents a conservative design stress level. The upper boundary of the shaded areas on the figure is set by the minimum jet nozzle area investigated, which was 2.26 square feet. This area setting

was chosen for investigation because it was the smallest area which would permit engine operation at the maximum coolant-flow ratio (about 0.05) at a turbine-inlet temperature less than 2060° R. As can be seen from the figure, operation at jet nozzle areas less than 2.26 square feet would be permissible at coolant flows lower than 0.05. Because the range of jet nozzle areas investigated was determined on the basis of engine performance with blade temperature range being only a secondary consideration, areas below 2.26 square feet were not covered in this investigation.

It can be seen from figure 11 that increased coolant-flow ratio effected a reduction in average blade temperature, but that the effectiveness of each percent of cooling air diminished as the coolant-flow ratio increased. For the range of engine operating conditions shown, the average blade temperature varied from about 1100° to 1150° F with no coolant to about 900° F at a coolant-flow ratio of 0.05. However, this increase in coolant-flow ratio is accompanied by a rise in turbine-inlet temperature ratio from about 3.4 to about 3.85 (temperature increases on the order of 250° F). If the band for a coolant-flow ratio of 0.01 were extrapolated to the limiting blade temperature line (stress-ratio factor of 2.3), it can be seen that operations at turbine-inlet temperature ratios up to about 3.6 (approximately 1868° R) would be permissible. Similar extrapolations at higher coolant-flow ratios which would permit higher turbine-inlet temperature ratios could be made, but the accuracy of the values obtained would be questionable without more operating data to indicate trends over the extrapolated region.

Temperatures existing in the rear half of the turbine rotor during operation at a jet nozzle area of 2.40 square feet varied from 960° R (500° F) at the hub to 1324° R (864° F) at the rim for zero coolant flow and from 860° R (400° F) at the hub to 1259° R (799° F) at the rim for a coolant-flow ratio of 0.05. The average temperature of the blade cooling air at the entrance to the blade base varied from 910° R (450° F) for the case of a coolant-flow ratio of 0.0489 to temperatures on the order of 1060° R (600° F) at very low coolant-flow ratios. This increase of cooling-air temperature with decrease in coolant-flow ratio is due to the heat added to the cooling air during the passage through the tail-cone struts, air supply tubes, and rotor impeller. In engines originally designed for turbine cooling, methods of introducing air to the turbine which do not use the high-temperature route through the tail cone would reduce the heat added to the cooling air before reaching the turbine rotor. This would increase the cooling effectiveness of the air and permit operation at lower coolant-flow ratios. Such methods of air introduction are discussed in reference 5.

Cooling air was bled from the compressor discharge rather than some other location on the compressor of this engine as a matter of convenience because bleed-off facilities existed at this point on this engine.

Reference 3 points out that, if permissible from the standpoint of cooling-air pressure, it is desirable to bleed off cooling air at an earlier stage. At a constant turbine-inlet temperature this earlier bleed-off point would result in a slight improvement in specific thrust and thrust specific fuel consumption. In addition to these advantages, the resulting lower cooling-air temperatures would reduce the required amount of bleed-off for cooling purposes.

The nature of the present provisional compressor bleed-off system was such that unduly large pressure drops in the cooling air were encountered. Comparison of the pressures at the compressor discharge and at the entrance to the rotor hub for the maximum coolant-flow ratios (tabulated in table I) will show the magnitude of these pressure drops at various engine speeds. Proper attention at the initial design of an air-cooled engine should greatly reduce these pressure drops. With such a design, higher coolant-flow ratios than those obtained in this investigation would be possible, or for the same range of coolant-flow ratios, the cooling-air supply could be bled from an earlier stage on the compressor. The losses in performance due to cooling that were measured in this engine were higher than necessary because of the high internal pressure losses of the cooling system and because compressor-discharge bleed-off required throttling losses in order to control the quantity of coolant flow.

## SUMMARY OF RESULTS

The following results were obtained in an investigation of the performance of an axial-flow-compressor turbojet engine equipped with a split-disk turbine rotor using air-cooled corrugated-insert rotor blades and provided with a cooling-air supply from a compressor-discharge bleed:

1. At a constant engine speed of about 7000 rpm and constant jet nozzle area of 2.40 square feet, turbine-inlet temperature ratio, specific thrust, and thrust specific fuel consumption all increased approximately linearly with increase in coolant-flow ratio. The percentage increases in these three parameters with increases in amount of cooling air bled from the compressor discharge are about 2.4 percent, 2.44 percent, and 1 percent, respectively, for each percent of coolant flow.

2. Comparisons of the measured (experimental) values of performance parameters from the present investigation with analytical values from a previous matching study on a similar engine show that the trends of the changes in the engine performance parameters with cooling for the two cases are similar.

3. Analytical calculations showed that, when an engine designed for air cooling is operated at fixed compressor conditions, a constant turbine-inlet temperature of 1760° R, and a constant turbine efficiency of 74 percent, each percent of cooling air bled from the compressor discharge will cause about a 3-percent decrease in specific thrust and about a 2-percent increase in thrust specific fuel consumption. If the turbine efficiency of this engine design were increased to 85 percent, each percent of cooling would then result in a 2-percent decrease in specific thrust and about a 1-percent increase in thrust specific fuel consumption. By increasing the turbine-inlet temperature to 2500° R, a further reduction in losses would occur, whereby each percent of cooling results in only a 1-percent decrease in specific thrust with the thrust specific fuel consumption remaining essentially constant.

4. Due to low turbine efficiencies, the starting and low-speed accelerating characteristics of this engine were very poor, and the turbine-inlet temperatures over the entire range of speeds investigated were higher than the design values.

5. The noncritical turbine rotor blades showed no signs of cracking, elongation, distortion, or erosion after about 52 hours of operation. Average blade temperatures measured during the investigation showed that the blades could be operated at 7000 rpm with a coolant-flow ratio of 0.01 and a turbine-inlet temperature of 1868° R (1408° F) to give a stress-ratio factor (ratio of average allowable blade stress-rupture strength to blade average centrifugal stress) of 2.3, which is considered a safe design value.

Lewis Flight Propulsion Laboratory
National Advisory Committee for Aeronautics
Cleveland, Ohio, December 21, 1954

## APPENDIX A

## SYMBOLS

The following symbols are used in this report:

| | |
|---|---|
| A | area, sq ft |
| $c_p$ | specific heat at constant pressure |
| F | thrust, lb |
| f/a | fuel-air ratio |
| g | standard gravitational acceleration, $ft/sec^2$ |
| $\overline{H}$ | lower heating value of fuel at $600^\circ$ R, Btu/lb |
| $\Delta H_t$ | total turbine work, Btu/sec |
| H/C | hydrogen-carbon ratio |
| h | enthalpy, Btu/lb |
| M | Mach number |
| N | rotational speed, rpm |
| p | pressure, in. Hg abs |
| R | gas constant, ft-lb/($^\circ$R)(lb) |
| T | temperature, $^\circ$F or $^\circ$R |
| w | weight flow, lb/sec |
| $w_f$ | fuel weight flow, lb/hr or lb/sec |
| $\gamma$ | ratio of specific heats |
| $\delta$ | pressure correction ratio, $p'/p'_0$ |
| $\eta$ | efficiency |
| $\theta$ | temperature correction ratio, $\dfrac{\frac{2\gamma}{\gamma+1}gRT'}{\left(\frac{2\gamma}{\gamma+1}gRT'\right)_0}$ |

Subscripts:

| | |
|---|---|
| b | burner |
| f | fuel |
| i | indicated |
| t | turbine |
| 0 | NACA sea-level standard; zero coolant-flow condition when used with engine performance parameters |
| 1 to 15 | measuring stations (see fig. 1) |

Superscript:

| | |
|---|---|
| ' | indicates total conditions |

# APPENDIX B

## CALCULATION PROCEDURE FOR DETERMINATION OF WEIGHT FLOW, TEMPERATURE, AND ENGINE PARAMETERS

### Calculation of Component Weight Flows

The various components of weight flow that make up the total engine weight flow were measured in the following ways (see fig. 1 for location and description of measuring stations):

| Quantity | Source | Purpose | Method of measuring |
|---|---|---|---|
| $w_f$ | Test-cell fuel lines | Fuel supply | Calibrated rotameter |
| $w_7$ | $w_{12}$ or $w_{13}$ | Turbine rotor and blade cooling | Instrument rake |
| $w_8$ | Compressor $8^{th}$ stage | Forward-rotor-face cooling | Sharp-edge orifice |
| $w_9$ | Compressor $12^{th}$ stage | Compressor balance | Pitot-static tube |
| $w_{10}$ | Compressor rear frame | Overboard vent for compressor rear seal | Sharp-edge orifice |
| $w_{11}$ | Compressor discharge | Rear-rotor-face cooling | Sharp-edge orifice |
| $w_{12}$ | Compressor discharge | Turbine rotor and blade cooling | Venturi |
| $w_{13}$ | Laboratory high-pressure air supply | Turbine rotor and blade cooling | Sharp-edge orifice |
| $w_{14}$ | Test-cell leakage | | Calibrated over a range of cell-to-ambient pressure differences |
| $w_{15}$ | Test-cell air intake | Engine air supply | Venturi |

Compressor-inlet weight flow $w_1$. - Compressor-inlet weight flow was calculated by two methods. The first method was a summation of component weight flows:

$$w_1 = w_{15} + w_{14} + w_9 + w_{10} \tag{B1}$$

Part of the compressor balance air $w_9$ passes directly into the first stage of the compressor and part leaks overboard and reenters the engine-inlet flow nozzle. However, the quantity of this flow is relatively small and does not appreciably affect the total quantity $w_1$. The second method was based on temperatures and pressures measured at station 1:

$$w_1 = p_1 A_1 M_1 \sqrt{\frac{\gamma_1 g}{RT_1}} \tag{B2}$$

where $M_1$ was obtained from table I of reference 16 for values of $p_1/p_1'$. The compressor-inlet temperature $T_1$ was determined from $T_i$ as described in the following section on temperature correction, and it is assumed that $T_1 = T_1'$ (valid for $M < 0.2$). The ratio of specific heats of the compressor inlet $\gamma_1$ was assumed to be 1.4. Weight flows measured by the two methods agreed within 1 percent over the range of engine speeds.

Turbine-inlet weight flow $w_3$. - Turbine-inlet weight flow was calculated by a summation of component weight flow as follows:

$$w_3 = w_{15} + w_{14} + w_f - w_8 - w_{11} - w_{12} \tag{B3}$$

The fuel-air ratio at the turbine inlet was determined as follows:

$$\left(\frac{f}{a}\right)_3 = \frac{w_f}{w_3 - w_f} \tag{B4}$$

## Temperature Determination

Correction to measured temperatures. - All temperatures were measured by means of thermocouples. In order to account for the recovery factor of the thermocouples, a calibration of the thermocouples was made in a free jet of air. A generalized relation between the total-to-static pressure ratio of the air jet and the ratio of the temperature error to the indicated temperature $((T' - T_i)/T_i)$ of the thermocouple was developed from this calibration, and all measured temperatures were corrected according to this relation to obtain a corrected measured temperature.

Calculated turbine-inlet temperature. - Because it was impractical to make a reasonable measurement of the average turbine-inlet temperature, this quantity was calculated from the method set forth in reference 17. Equation (8) of this reference, when rewritten in the nomenclature of this report, is

$$h_3 = \frac{\eta_b \frac{f}{a} \overline{H} + h_2 + \frac{f}{a} h_f}{1 + \frac{f}{a}} \tag{B5}$$

where $\overline{H} = 15{,}935 + 15{,}800(H/C)$ from reference 17 and $H/C = 0.169$ for the fuel used. The burner efficiency $\eta_b$ was assumed to be 0.98, and the value of $h_f$ was considered negligible. From this value of $h_3$, the turbine-inlet temperature $T'_3$ can be determined from chart II of reference 17.

## Engine Performance Parameters

Corrected specific thrust. - Corrected specific thrust is defined as $F/w_1\sqrt{\theta_1}$. The thrust $F$ was measured by a strain-gage thrust link and was also calculated by the method indicated in appendix B of reference 4. Because the test cell and the exhaust muffler (see fig. 1) were at different pressure levels (pressure higher in the muffler), there was a net force exerted on the engine. The magnitude of this force was calibrated over a range of engine thrust and cell-to-muffler pressure differences. The indicated thrust from the strain-gage reading was corrected by subtracting the force due to this pressure difference. Also, due to this same pressure difference between cell and muffler, the expansion across the jet nozzle was not as great as would occur in an engine operating in free air. This decrease in thrust was accounted for by adding to the indicated thrust the product of the tail-pipe area and the pressure difference. The indicated thrust with the two aforementioned thrust corrections yields the measured thrust of the engine. Only the second of the two thrust corrections mentioned was necessary to correct the calculated thrust.

The measured and calculated thrust agreed within 2 percent over the range of engine speeds. The measured thrust and the compressor-inlet weight flow determined by equation (1), after correction of both to standard sea-level conditions, were used to determine values of specific thrust for the present report.

Corrected thrust specifuc fuel consumption. - Corrected thrust specific fuel consumption is defined as $w_f/F\sqrt{\theta_1}$. The fuel consumption

$w_f$, as measured by a calibrated rotameter, was corrected to standard sea-level conditions $w_f/\delta_1\sqrt{\theta_1}$. The corrected measured thrust $F/\delta_1$, as determined in the preceding section, was used in conjunction with the corrected fuel consumption to determine the corrected thrust specific fuel consumption $w_f/F\sqrt{\theta_1}$.

## REFERENCES

1. Schramm, Wilson B., Nachtigall, Alfred J., and Arne, Vernon L.: Preliminary Analysis of Effects of Air Cooling Turbine Blades on Turbojet-Engine Performance. NACA RM E50E22, 1950.

2. Hubbartt, James E., Rossbach, Richard J., and Schramm, Wilson B.: Analysis of Factors Affecting Selection and Design of Air-Cooled Single-Stage Turbines for Turbojet Engines. III - Engine Design-Point Performance. NACA RM E54F16a, 1954.

3. Esgar, Jack B., and Ziemer, Robert R.: Effects of Turbine Cooling with Compressor Air Bleed on Gas-Turbine Engine Performance. NACA RM E54L20, 1955.

4. Ziemer, Robert R., Schafer, Louis J., Jr., and Heaton, Thomas R.: Performance of Two Air-Cooled Turbojet Engines Determined Analytically from Engine Component Performance for a Range of Cooling-Air Weight Flows. NACA RM E53K19, 1954.

5. Moseson, Merland L., Krasner, Morton H., and Ziemer, Robert R.: Mechanical Design Analysis of Several Noncritical Air-Cooled Turbine Disks and a Corrugated-Insert Air-Cooled Turbine Rotor Blade. NACA RM E53E21, 1953.

6. Kemp, Richard H., and Moseson, Merland L.: Investigations of Air-Cooled Turbine Rotors for Turbojet Engines. II - Mechanical Design, Stress Analysis, and Burst Test of Modified J33 Split-Disk Rotor. NACA RM E51J03, 1952.

7. Heaton, Thomas R., Slivka, William R., and Westra, Leonard F.: Cold-Air Investigation of a Turbine with Nontwisted Rotor Blades Suitable for Air Cooling. NACA RM E52A25, 1952.

8. Slivka, William R., and Silvern, David H.: Analytical Evaluation of Aerodynamic Characteristics of Turbines with Nontwisted Rotor Blades. NACA TN 2365, 1951.

9. Bartoo, Edward R., and Clure, John L.: Experimental Investigation of Air-Cooled Turbine Blades in Turbojet Engine. XII - Cooling Effectiveness of a Blade with an Insert and with Fins Made of a Continuous Corrugated Sheet. NACA RM E52F24, 1952.

10. Ziemer, Robert R., and Slone, Henry O.: Analytical Procedures for Rapid Selection of Coolant Passage Configurations for Air-Cooled Turbine Rotor Blades and for Evaluation of Heat-Transfer, Strength, and Pressure-Loss Characteristics. NACA RM E52G18, 1952.

11. Bartoo, Edward R., and Clure, John L.: Experimental Investigation of Air-Cooled Turbine Blades in Turbojet Engine. XIII - Endurance Evaluation of Several Protective Coatings Applied to Turbine Blades of Nonstrategic Steels. NACA RM E53E18, 1953.

12. Stepka, Francis S., Bear, H. Robert, and Clure, John L.: Experimental Investigation of Air-Cooled Turbine Blades in Turbojet Engine. XIV - Endurance Evaluation of Shell-Supported Turbine Rotor Blades Made of Timken 17-22A(S) Steel. NACA RM E54F23a, 1954.

13. Smith, Gordon T., and Curren, Arthur N.: Comparison of Pressure-Loss Characteristics of Several Tail-Cone Air-Induction Systems for Air-Cooled Gas-Turbine Rotors. NACA RM E52K07, 1953.

14. Esgar, Jack B., and Ziemer, Robert R.: Methods for Rapid Graphical Evaluation of Cooled or Uncooled Turbojet and Turboprop Engine or Component Performance (Effects of Variable Specific Heat Included). NACA TN 3335, 1955.

15. Reeman, J., and Buswell, R. W. A.: An Experimental Single-Stage Air-Cooled Turbine. Pt. I. Design of the Turbine and Manufacture of Some Experimental Internally Cooled Nozzles and Blades. Proc. A, Inst. Mech Eng., vol. 167, no. 4, 1953, pp. 341-350; discussion, pp. 363-370.

16. Ames Research Staff: Equations, Tables, and Charts for Compressible Flow. NACA Rep. 1135, 1953. (Supersedes NACA TN 1428.)

17. English, Robert E., and Wachtl, William W.: Charts of Thermodynamic Properties of Air and Combustion Products from 300° to 3500° R. NACA TN 2071, 1950.

TABLE I. - SUMMARY OF ENGINE OPERATING CONDITIONS

| Series | Engine speed, N, rpm | Compressor-inlet total temperature, $T_1'$, °R | Compressor-inlet total pressure, $p_1'$, in. Hg abs | Compressor-inlet air flow, $w_1$, lb/sec | Compressor-discharge total temperature, $T_2'$, °R | Compressor-discharge total pressure, $p_2'$, in. Hg abs | Calculated turbine-inlet total temperature, $T_3'$, °R | Fuel flow, $w_f$, lb/sec | Jet nozzle area, $A_6$, sq ft | Measured thrust, F, lb | Coolant-flow ratio, $w_7/w_1$ | Cooling-air total pressure at turbine rotor hub, $p_7'$, in. Hg abs |
|---|---|---|---|---|---|---|---|---|---|---|---|---|
| A | 4840 | 509 | 29.34 | 50.86 | 666 | 64.22 | 1615 | 0.64 | 2.40 | 1309 | 0.0501 | 36.89 |
| | 4826 | 509 | 29.34 | 50.48 | 666 | 64.03 | 1572 | .61 | | 1269 | .0396 | 32.99 |
| | 4840 | 509 | 29.34 | 50.66 | 666 | 64.44 | 1538 | .59 | | 1239 | .0270 | 29.40 |
| B | 5882 | 502 | 29.38 | 75.15 | 742 | 96.49 | 1600 | .86 | | 2599 | .0480 | 50.18 |
| | 5887 | 503 | 29.35 | 74.21 | 743 | 94.96 | 1582 | .84 | | 2523 | .0377 | 41.08 |
| | 5883 | 503 | 29.35 | 74.50 | 744 | 95.57 | 1557 | .82 | | 2480 | .0281 | 35.01 |
| | 5884 | 503 | 29.36 | 74.71 | 744 | 95.65 | 1530 | .80 | | 2450 | .0193 | 31.08 |
| | 5978 | 515 | 29.10 | 73.30 | 765 | 95.26 | 1511 | .76 | | 2287 | 0 | ----- |
| C | 6944 | 516 | 28.89 | 89.38 | 838 | 124.29 | 1959 | 1.38 | | 4258 | .0492 | 63.94 |
| | 6932 | 513 | 29.07 | 90.48 | 835 | 124.44 | 1929 | 1.35 | | 4232 | .0489 | 64.23 |
| | 6889 | 506 | 29.22 | 91.97 | 821 | 126.61 | 1915 | 1.39 | | 4314 | .0493 | 65.65 |
| | 6929 | 513 | 29.08 | 90.50 | 831 | 125.02 | 1893 | 1.33 | | 4147 | .0394 | 52.87 |
| | 6929 | 514 | 29.07 | 90.49 | 833 | 124.76 | 1845 | 1.28 | | 4034 | .0307 | 44.14 |
| | 6927 | 513 | 29.07 | 90.39 | 834 | 124.70 | 1822 | 1.25 | | 3976 | .0237 | 39.22 |
| | 6928 | 513 | 29.07 | 90.38 | 835 | 124.82 | 1800 | 1.23 | | 3925 | .0170 | 35.94 |
| | 6971 | 520 | 28.96 | 89.09 | 845 | 124.55 | 1761 | 1.15 | | 3720 | 0 | ----- |
| D | 6941 | 520 | 28.88 | 90.19 | 844 | 125.98 | 1965 | 1.40 | 2.32 | 4381 | .0493 | 64.99 |
| | 6938 | 519 | 28.89 | 90.43 | 843 | 126.12 | 1921 | 1.36 | | 4262 | .0388 | 51.95 |
| | 6947 | 520 | 28.88 | 90.25 | 843 | 126.28 | 1880 | 1.31 | | 4178 | .0298 | 43.21 |
| | 6938 | 520 | 28.87 | 89.86 | 842 | 125.88 | 1840 | 1.27 | | 4073 | .0190 | 37.22 |
| E | 6944 | 519 | 28.88 | 89.86 | 848 | 127.62 | 2039 | 1.49 | 2.26 | 4603 | .0502 | 65.98 |
| | 6943 | 519 | 28.88 | 89.97 | 847 | 126.81 | 1985 | 1.43 | | 4459 | .0395 | 52.68 |
| | 6938 | 520 | 28.88 | 90.28 | 845 | 127.38 | 1922 | 1.37 | | 4313 | .0286 | 43.00 |
| | 6938 | 519 | 28.87 | 90.19 | 846 | 127.77 | 1886 | 1.33 | | 4276 | .0195 | 39.12 |
| F | 7836 | 506 | 29.16 | 103.1 | 890 | 154.05 | 2314 | 2.10 | 2.40 | 6082 | .0314 | 51.87 |

| Station | Description | Quantities measured |
|---|---|---|
| 1 | Compressor inlet | $p, p', T'_i$ |
| 2 | Compressor discharge | $p, p', T'_i$ |
| 3 | Turbine inlet | $p', T'_i$ |
| 4 | Turbine discharge | $p, p', T'_i$ |
| 5 | Tail pipe | $p, p', T'_i$ |
| 6 | Jet nozzle | $p$ |
| 7 | Cooling air entering rotor | $p, p', T'_i$ |
| 8 | Compressor eighth-stage bleed (cooling air for forward face of turbine) | $p, \Delta p, T'_i$ |
| 9 | Compressor balance air | $p, p', T'_i$ |
| 10 | Compressor overboard bleed | $p, \Delta p, T'_i$ |
| 11 | Compressor-discharge bleed (cooling air for rear face of turbine) | $p, \Delta p, T'_i$ |
| 12 | Compressor-discharge bleed for blade cooling air | $p, \Delta p, T'_i$ |
| 13 | External supply for blade cooling air | $p, \Delta p, T'_i$ |
| 14 | Test-cell leakage | $p, \Delta p, T'_i$ |
| 15 | Test-cell air inlet | $p, \Delta p, T'_i$ |

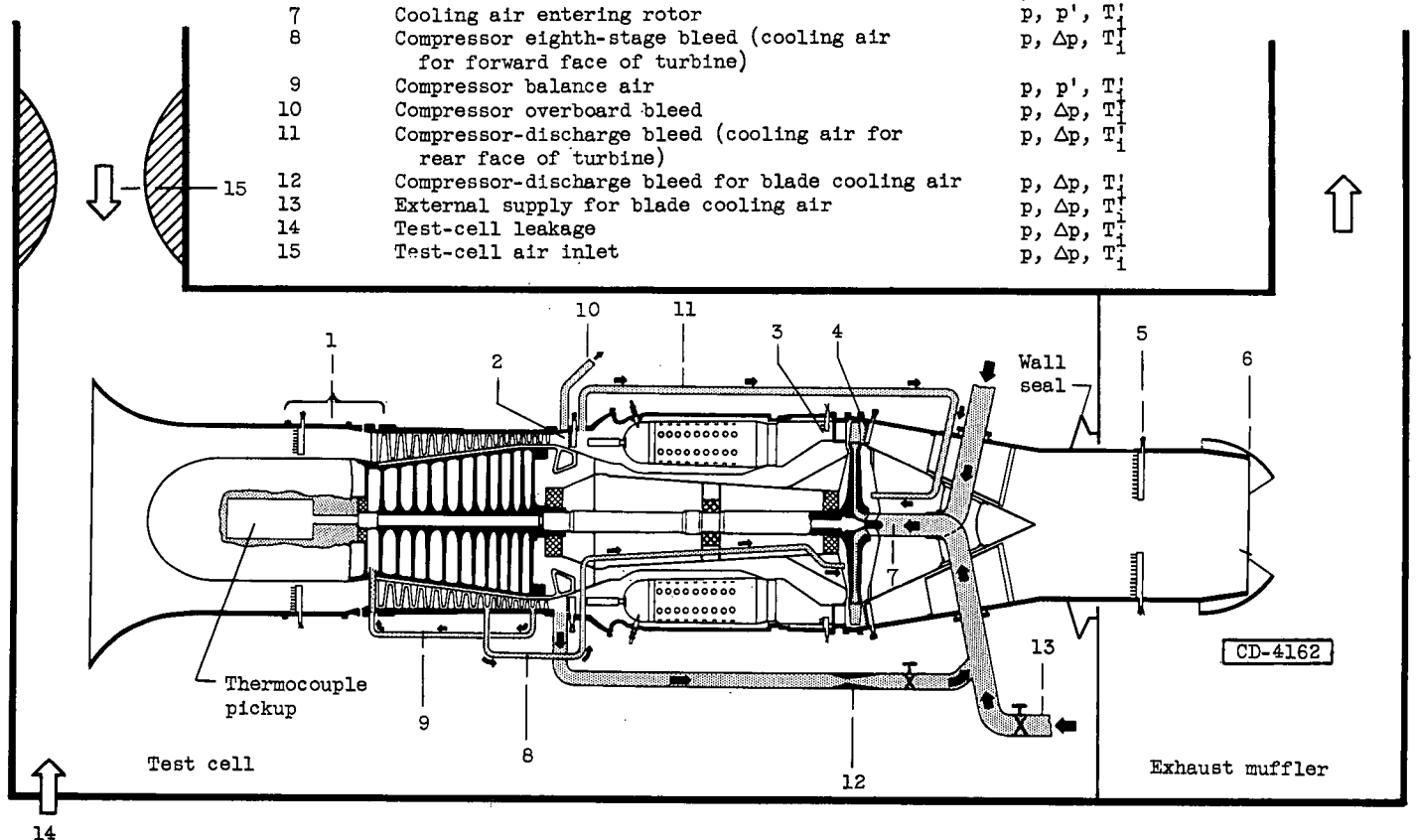


Figure 1. - Schematic diagram of production-model axial-flow-compressor turbojet engine modified for turbine cooling with compressor-discharge bleed-off showing measuring stations and piping layout.

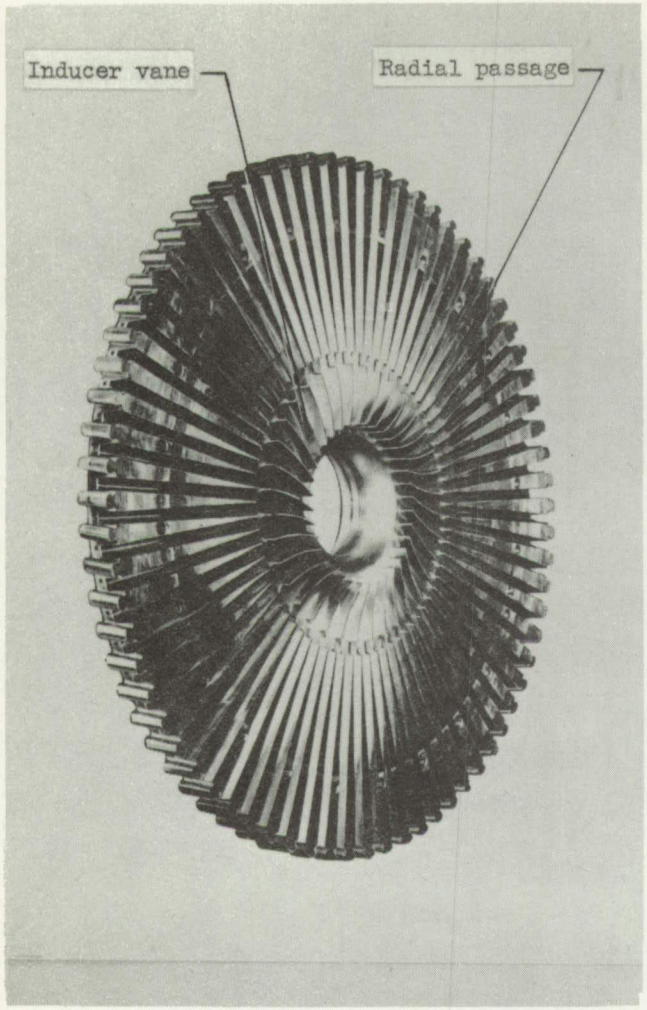


(a) Interior view of rear half.

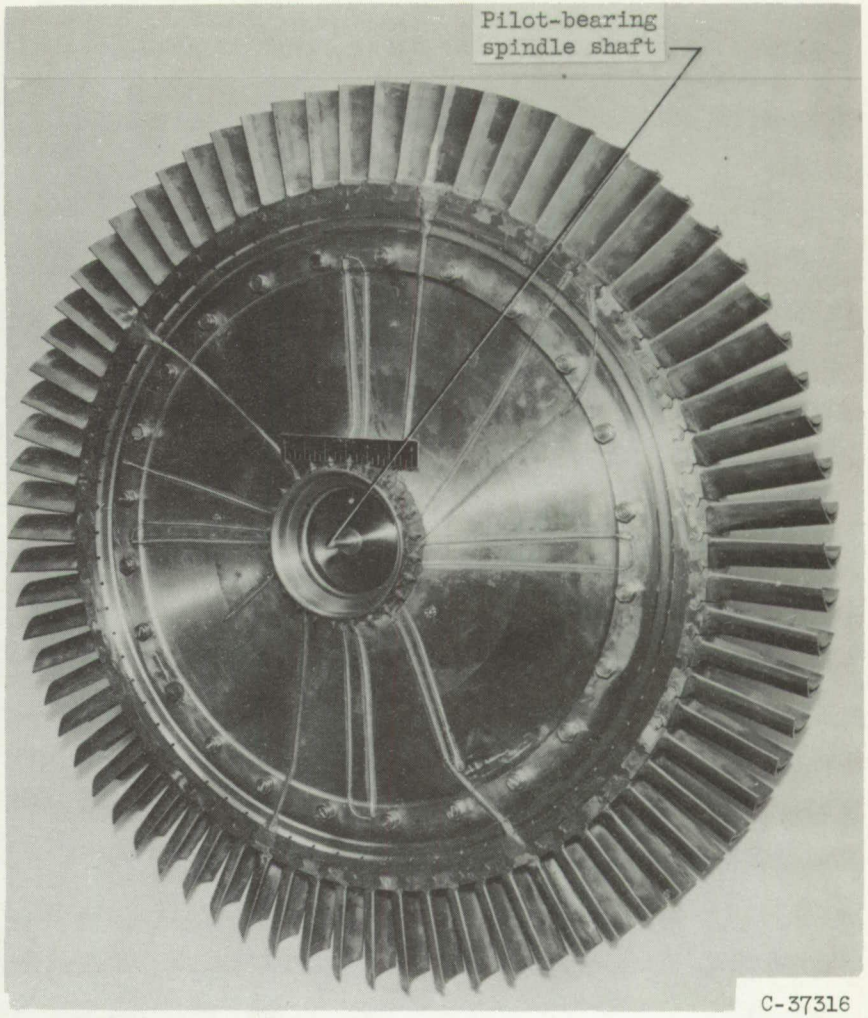


(b) Exterior view (rear face) of assembled rotor.

Figure 2. - Split-disk air-cooled turbine rotor for modified-production-model axial-flow-compressor turbojet engine.

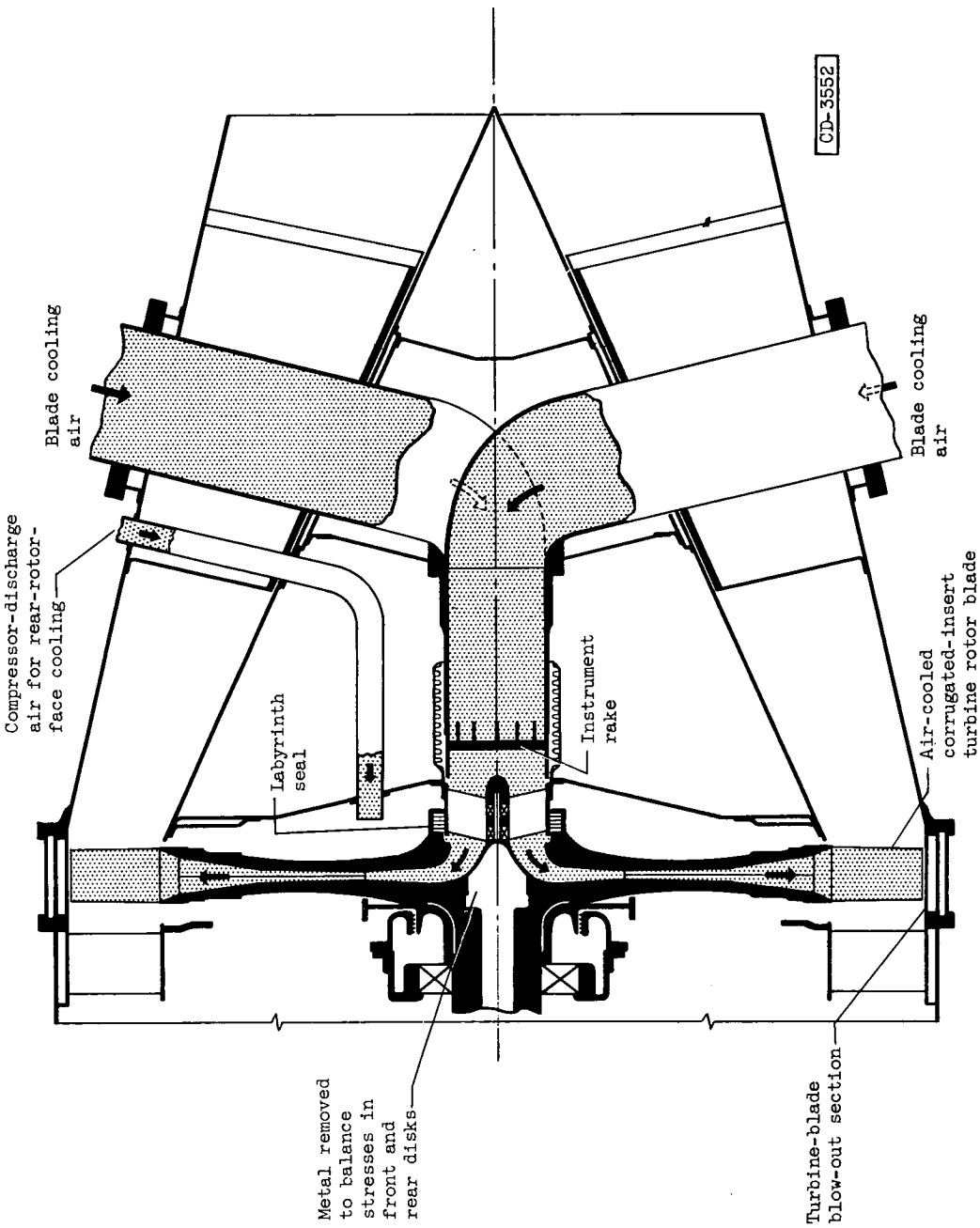


Figure 3. - Modified tail cone showing cooling-air entry for split-type air-cooled turbine rotor.

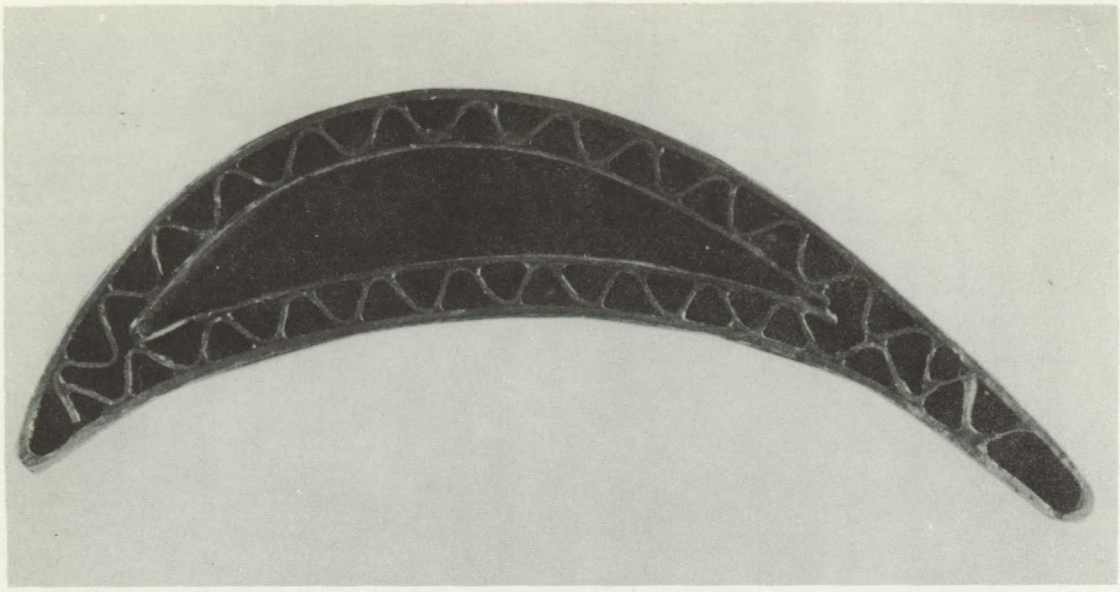

(a) Tip view.

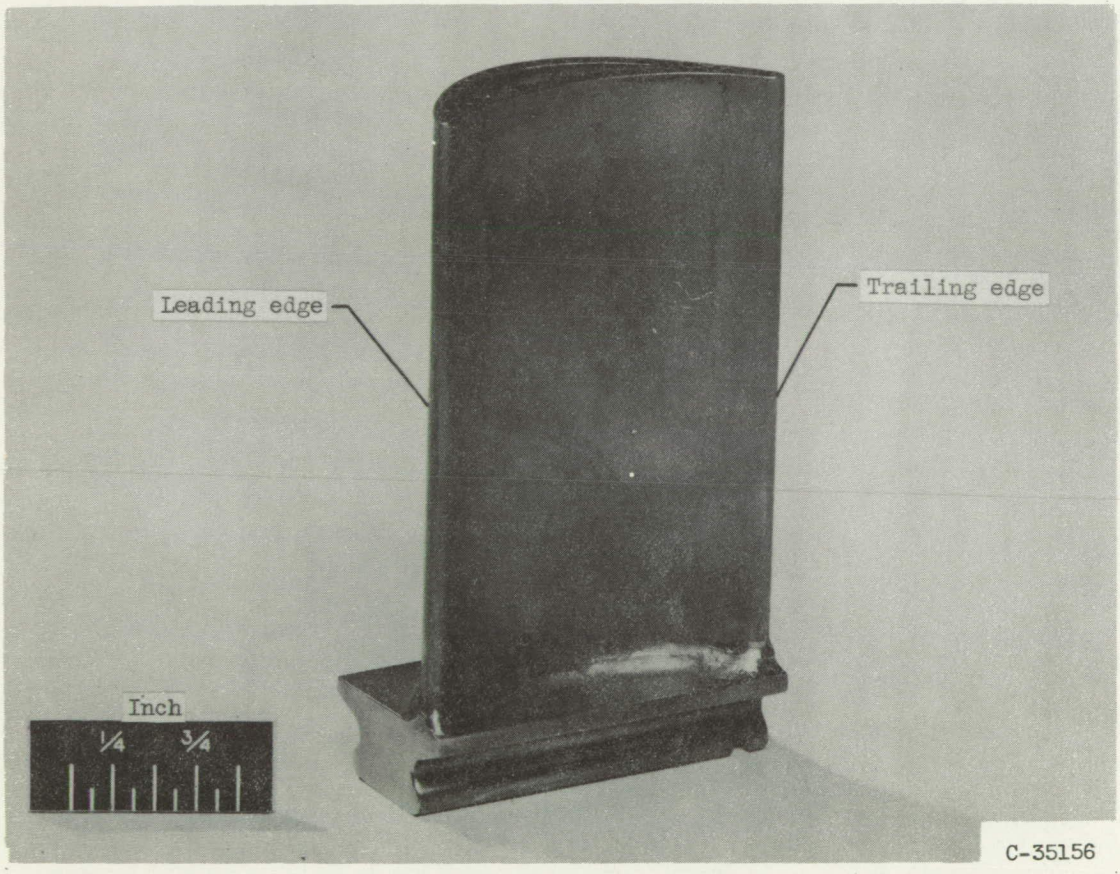


(b) Side view (pressure surface).

Figure 4. - Air-cooled corrugated-insert turbine rotor blade for modified engine.

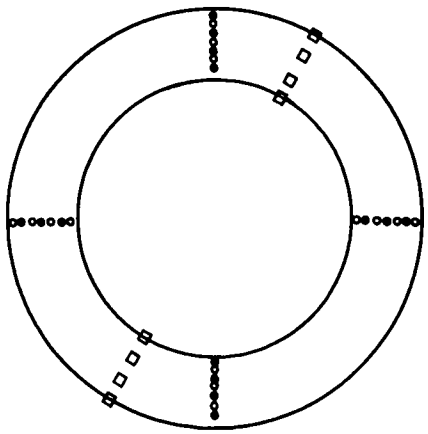

(a) Compressor inlet, station 1.

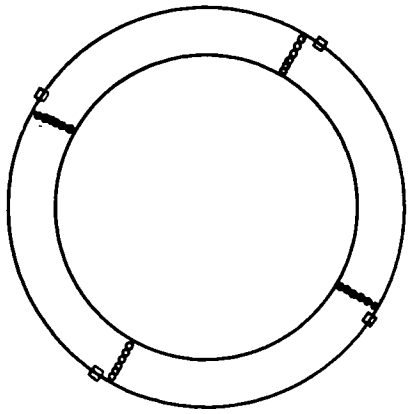

(b) Compressor discharge, station 2.

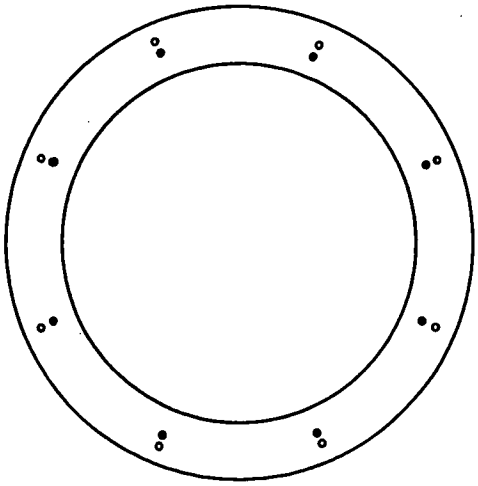

(c) Turbine inlet, station 3.

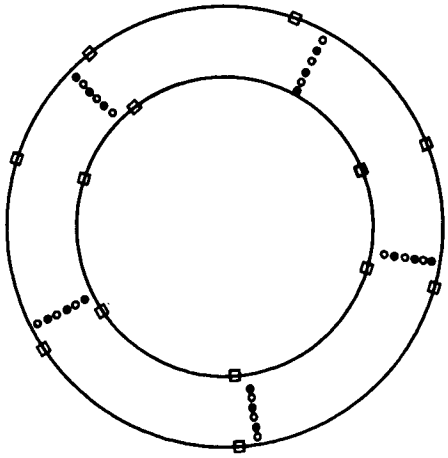

(d) Turbine discharge, station 4.

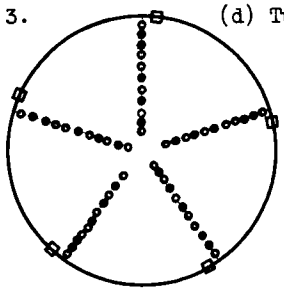

(e) Tail pipe, station 5.

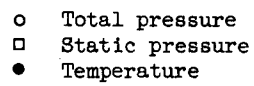


Figure 5. - Temperature and pressure surveys installed at measuring stations in engine.

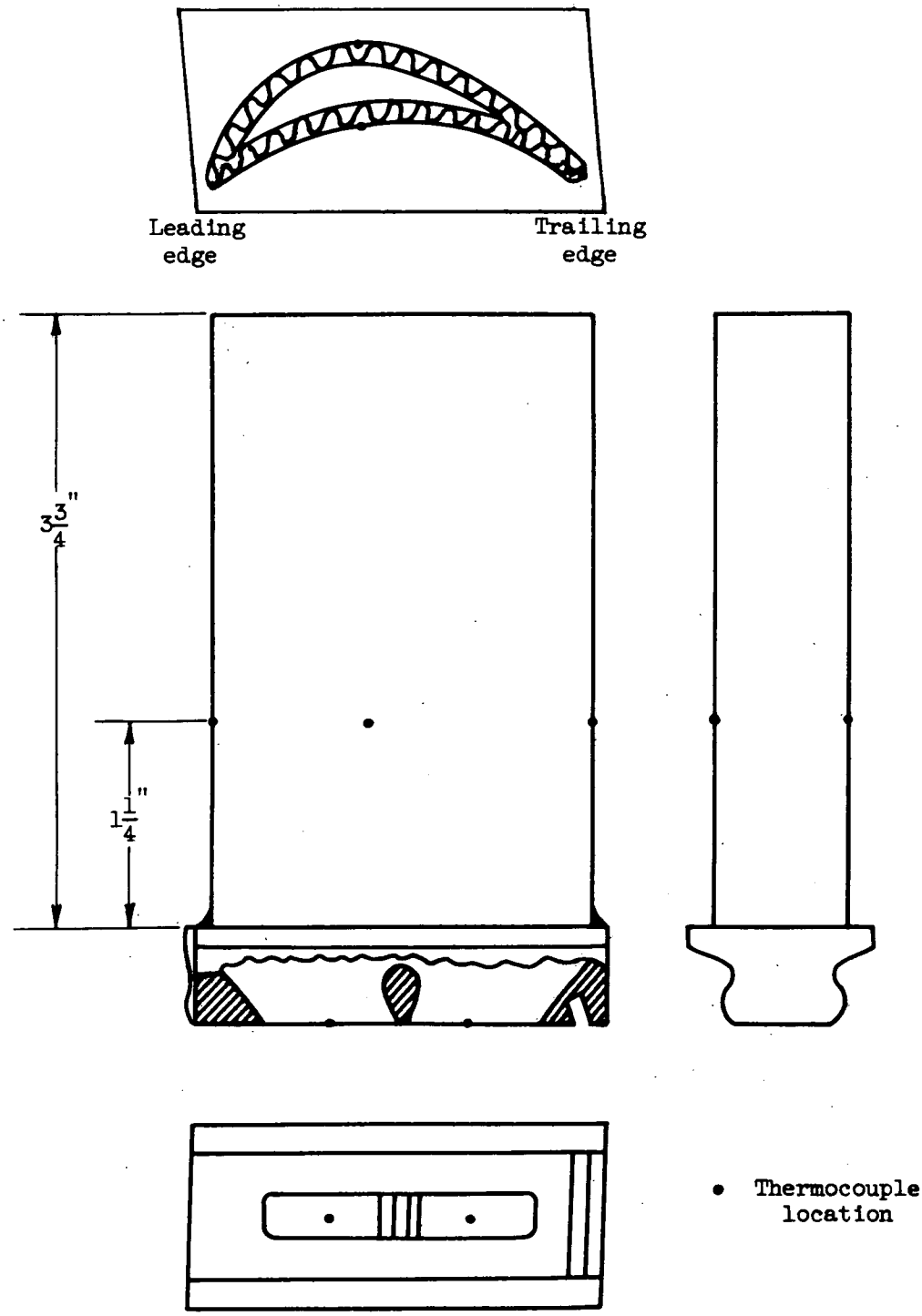


Figure 6. - Location of thermocouples for rotor-blade temperature distribution.

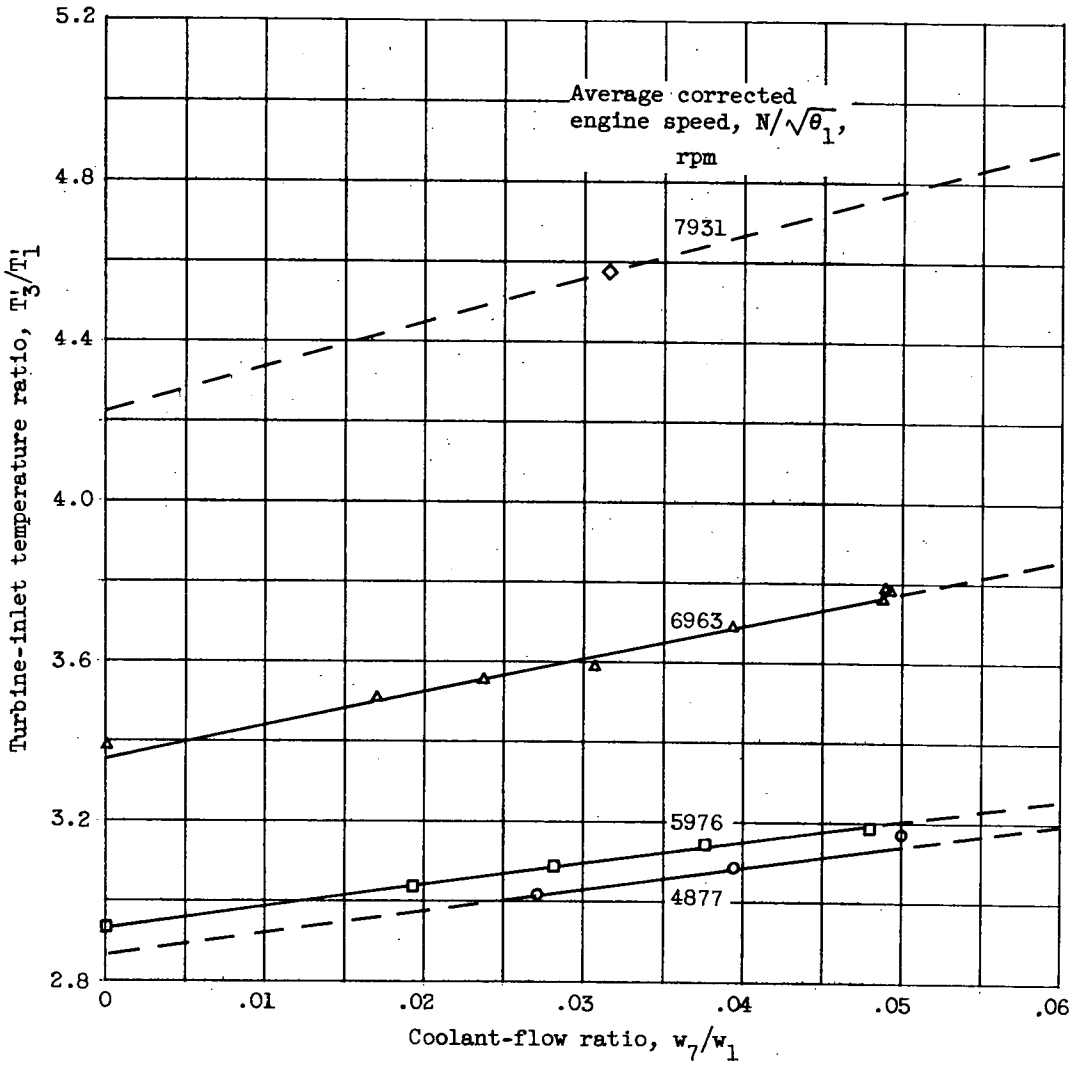


(a) Turbine-inlet temperature ratio.

Figure 7. - Variation of engine performance with coolant-flow ratio over range of corrected engine speeds at jet nozzle area of 2.40 square feet.

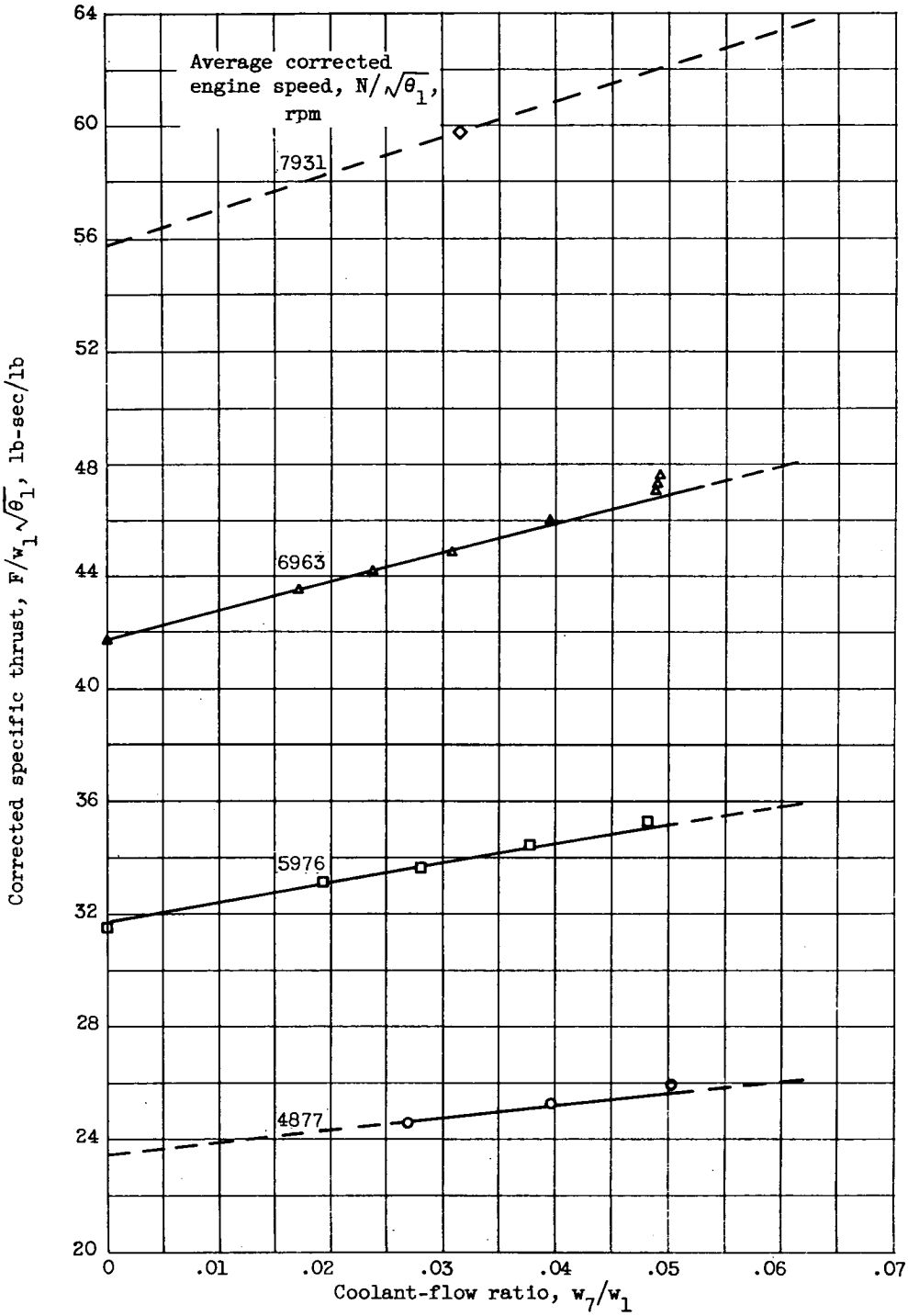


(b) Corrected specific thrust.

Figure 7. - Continued. Variation of engine performance with coolant-flow ratio over range of corrected engine speeds at jet nozzle area of 2.40 square feet.

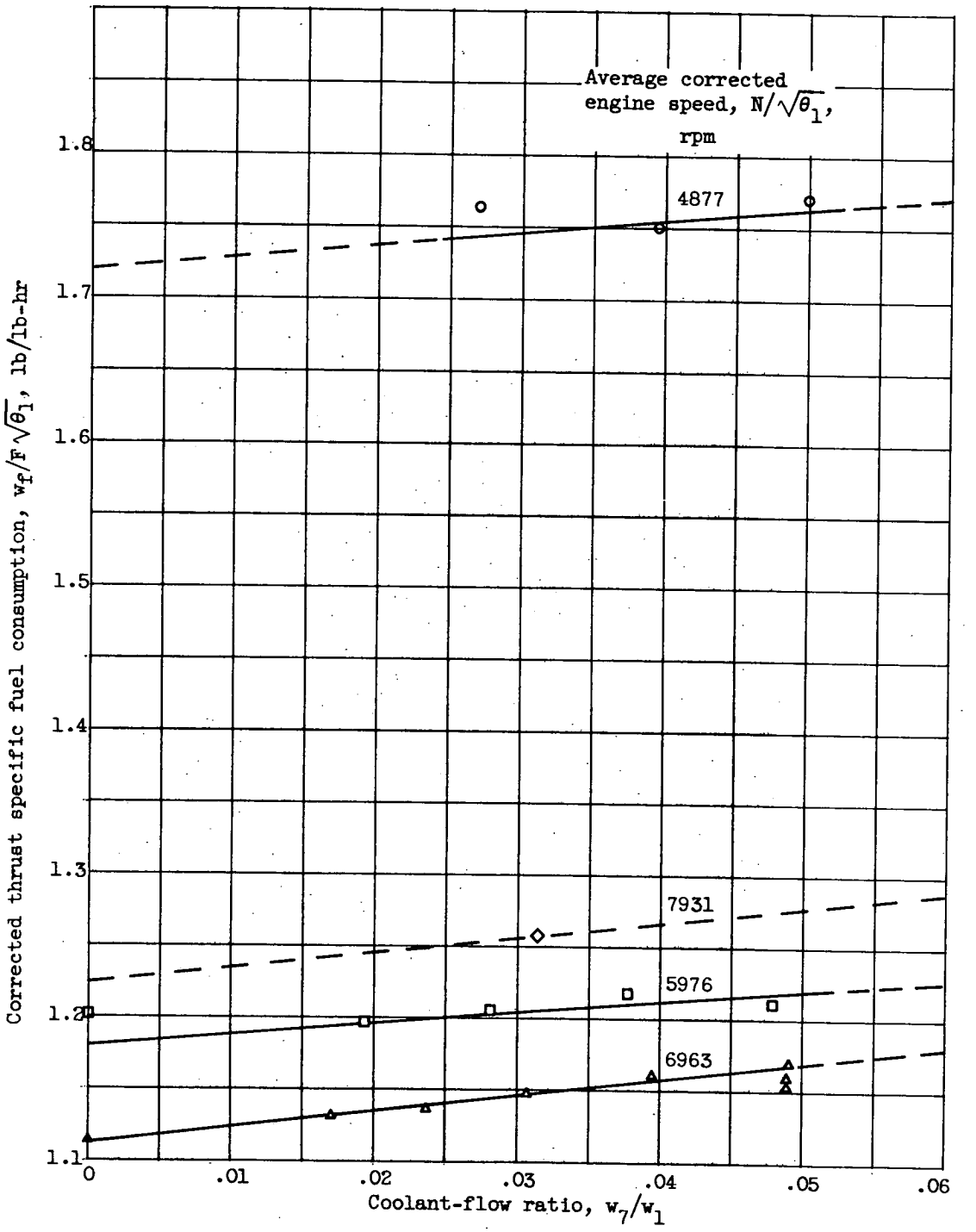


(c) Corrected thrust specific fuel consumption.

Figure 7. - Concluded. Variation of engine performance with coolant-flow ratio over range of corrected engine speeds at jet nozzle area of 2.40 square feet.

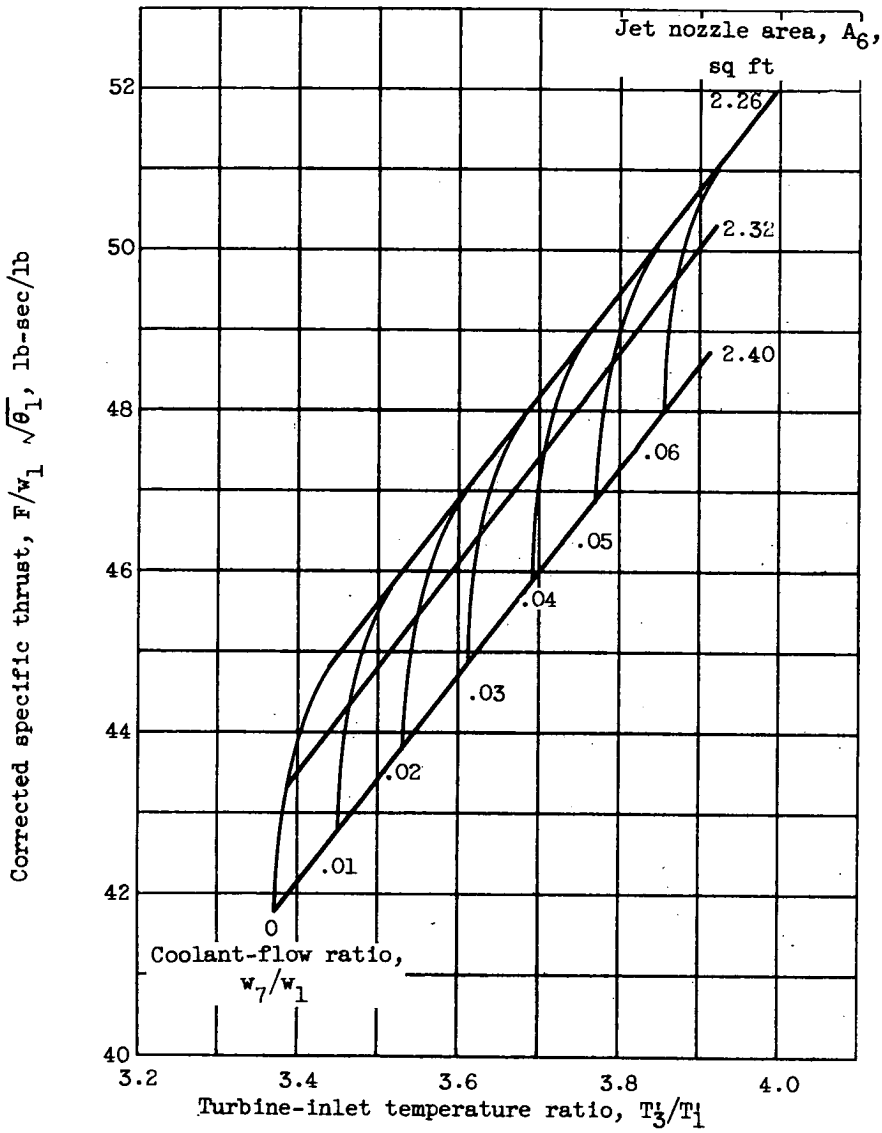


(a) Corrected specific thrust.

Figure 8. - Variation of engine performance with turbine-inlet temperature ratio at corrected engine speed of 7000 rpm for ranges of coolant-flow ratios and jet nozzle areas.

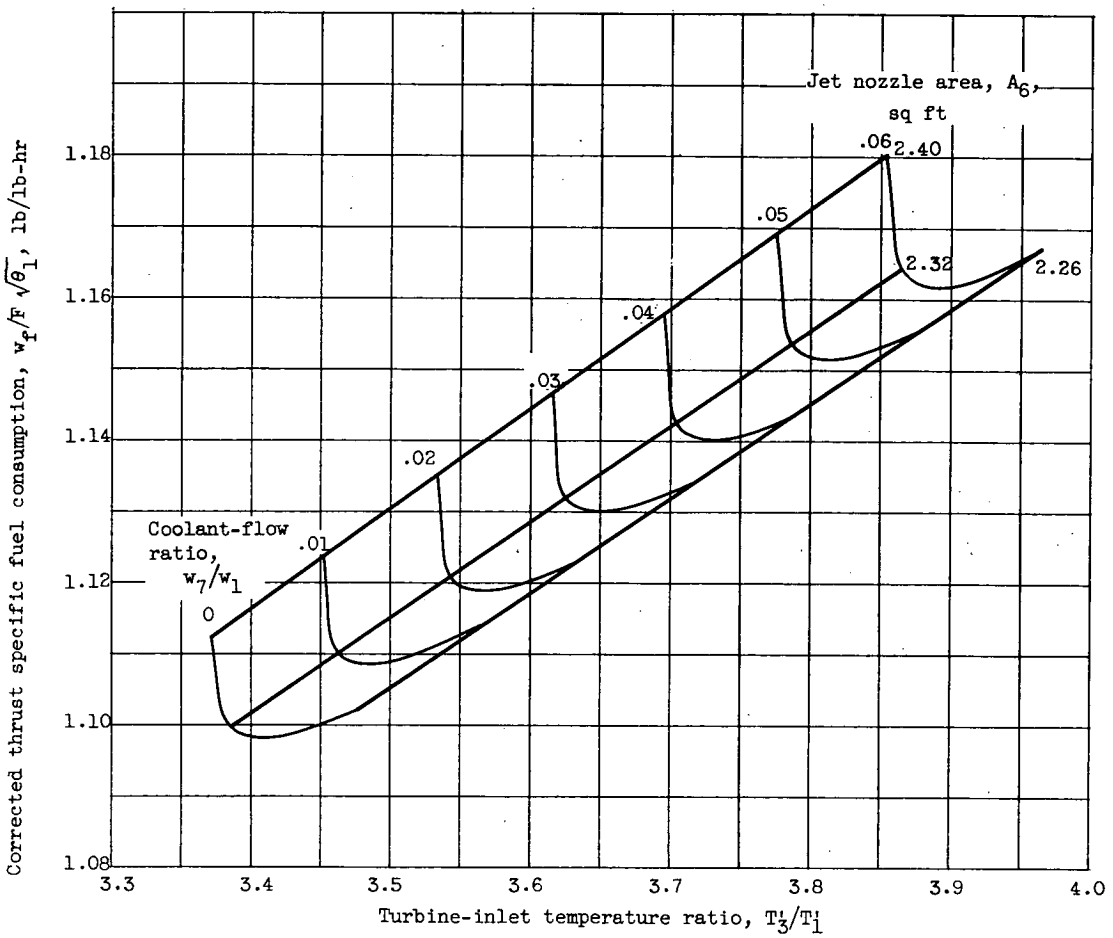


(b) Corrected thrust specific fuel consumption.

Figure 8. - Concluded. Variation of engine performance with turbine-inlet temperature ratio at corrected engine speed of 7000 rpm for ranges of coolant-flow ratios and jet nozzle areas.

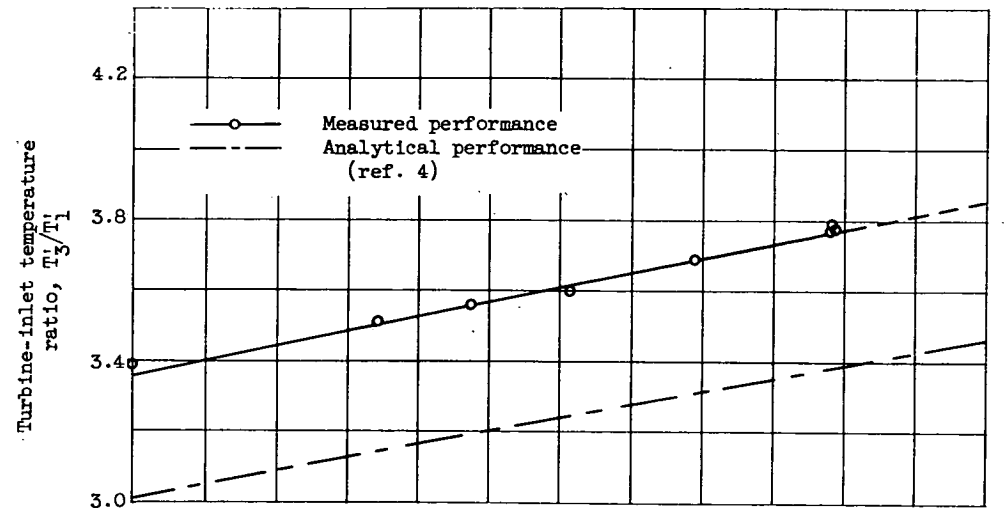


(a) Turbine-inlet temperature ratio.

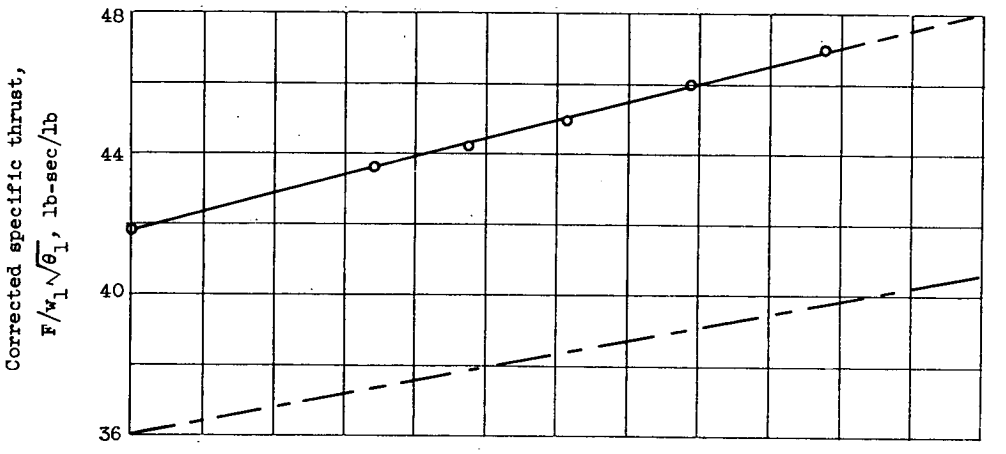


(b) Corrected specific thrust.

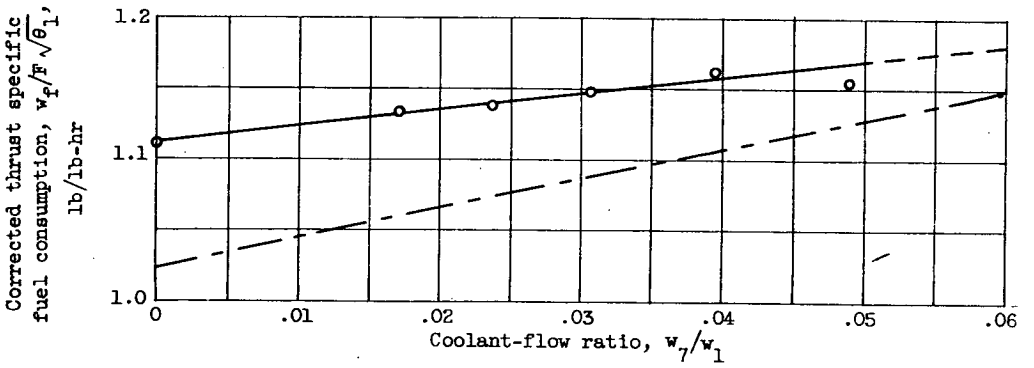


(c) Corrected thrust specific fuel consumption.

Figure 9. - Comparison of analytical and measured variations in engine performance parameters with coolant-flow ratio at corrected engine speed of 6963 rpm and jet nozzle area of 2.40 square feet.

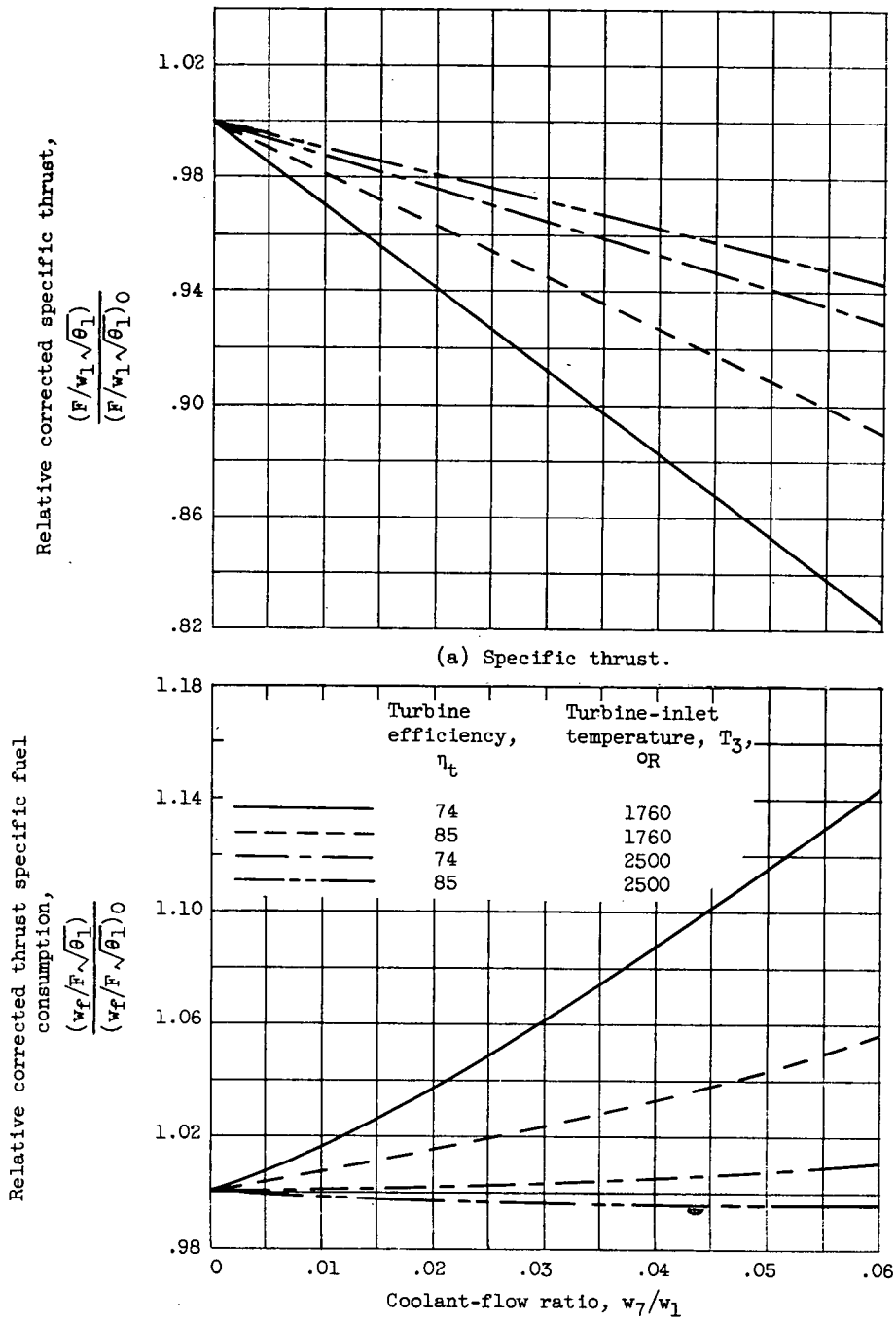


(a) Specific thrust.

(b) Thrust specific fuel consumption.

Figure 10. - Analytical predictions of air-cooled engine performance at corrected engine speed of 7000 rpm and various turbine-inlet temperatures and turbine efficiencies.

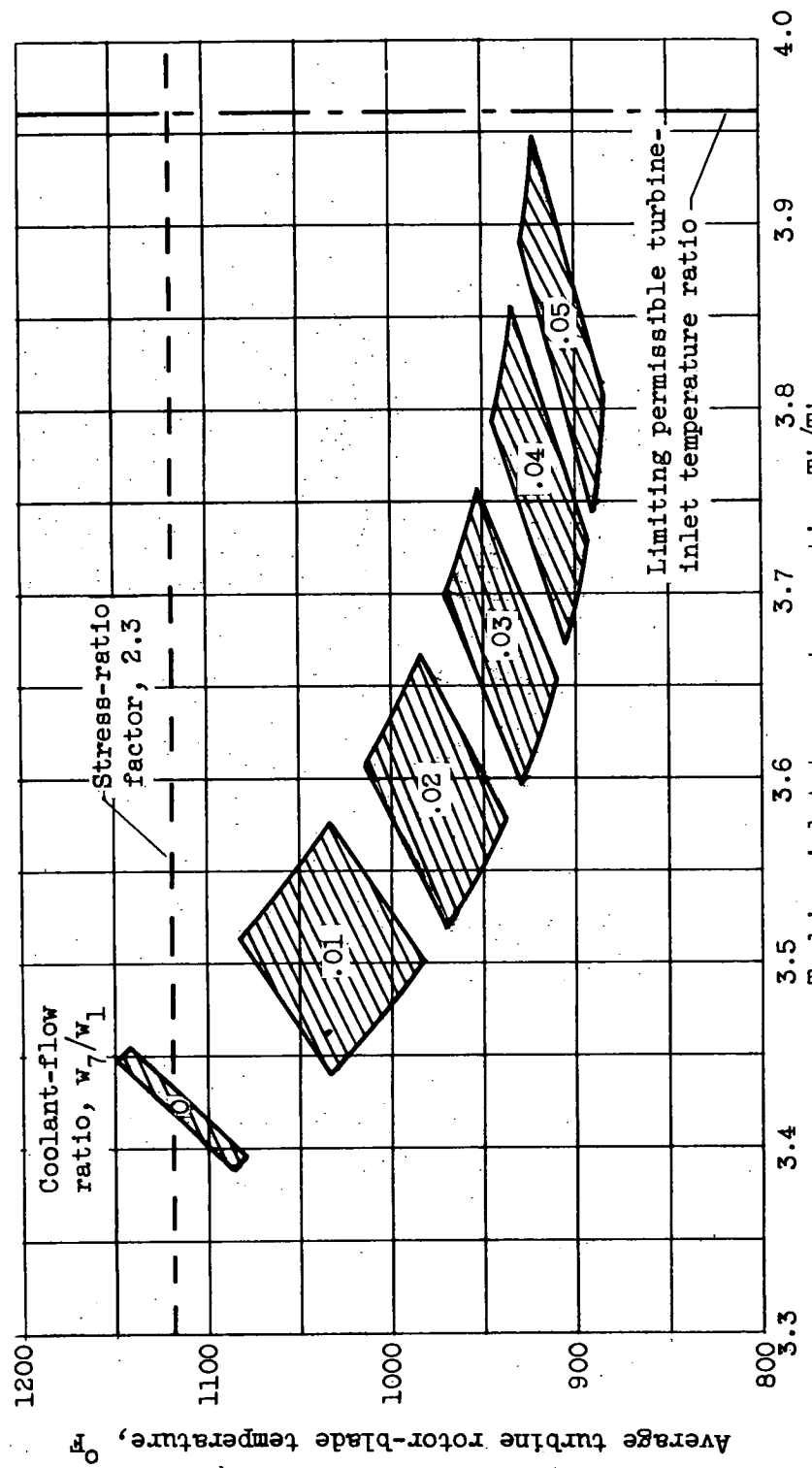


Figure 11. - Variation of average turbine rotor-blade temperature with turbine-inlet temperature ratio for range of coolant-flow ratios at 7000 rpm.